Control of line tension at phase-separated domain boundary in lipid membranes

NICHAPORN WONGSIROJKUL

JAPAN ADVANCED INSTITUTE OF SCIENCE AND TECHNOLOGY

SEPTEMBER 2020

Doctoral Dissertation

Control of line tension at phase-separated domain boundary in lipid membranes

NICHAPORN WONGSIROJKUL

Supervisor: Professor TAKAGI Masahiro

Graduate School of Advanced Science and Technology
Japan Advanced Institute of Science and Technology
[Materials Science]
(September 2020)

Abstract

[Background]

Lipid bilayer membrane is the basic structure of cell membrane which is the boundary between inside and outside regions of a cell. Cell membranes have lateral heterogeneity consisting of various lipids, proteins, glycolipids, and glycoproteins. From the raft hypothesis, raft regions mainly consisting of sphingolipids and cholesterol are believed to regulate membrane-protein interaction, cell signaling, and membrane trafficking by modulating the lateral organization of the membrane. Phospholipids in water naturally assemble into the bilayer structure by hydrophobic interactions. Interestingly, phase separation can occur in the artificial multicomponent lipid bilayers. The typical phases at room temperature are a solid-ordered (S_o) phase which is rich in saturated lipids, a liquid-ordered (L_o) phase which is rich in saturated lipids and cholesterol, and liquid-disordered (L_d) phase composed largely of unsaturated lipids.

It is important to consider the interfacial tension at the phase-separated domain boundary (line tension) when we discuss the stability of phase separation. Generally, as the line tension becomes smaller, the domain size becomes smaller, the domains start to fluctuate, and the phase separation disappears finally. Therefore, the control of line tension leads to the control of phase-separated structures.

In this thesis, the line tension is controlled by two methods. First one is osmotic swelling. The response of cells and their phase behaviors to the osmotic stress is important for cell homeostasis and survival in several body systems, particularly in the circulation system. It was reported that osmotic swelling can enhance the phase separation to occur. In other words, the osmotic swelling may increase the line tension. However, the physicochemical mechanism behind still unclear. Second method is the addition of unsaturated fatty acids. Unsaturated fatty acids decrease the high-density lipoprotein cholesterol and may decrease the risk of cardiovascular disease. Also, Oleic acid, one of unsaturated fatty acids, decreases the line tension at liquid domain boundary. It is expected that the more precise control of phase separation becomes possible by combining these two methods.

[Objective]

In this thesis, we investigated the effects of osmotic pressure on phase separation and miscibility temperature in lipid membranes consisting of dioleolylphosphocholine (DOPC)/ dipalmitoylphosphocholine (DPPC)/ Cholesterol (Chol). The line tension analysis at the domain boundary of DOPC/DPPC/Chol and diphytanoylphosphatidylcholine (DiphyPC)/DPPC/Chol were also compared. In the last part, we showed the modulate of the line tension in the fatty acids mixed DOPC/DPPC/Chol membrane. Also, the changes of line tension in fatty acids-containing lipid membranes by osmotic pressure were examined.

[Results]

It was found that the application of osmotic pressure can widen the area of phase-separated in the phase diagram and increase the miscibility temperature which is a transition temperature between phase separation and homogeneous phase. Interestingly, we found that miscibility temperature increased greater at the higher cholesterol concentration. Furthermore, osmotic pressure can increase the line tension at the domain boundary in both DOPC/DPPC/Chol and DiphyPC/DPPC/Chol systems similarly. The plausible mechanism behind was also proposed that the osmotic pressure mediated membrane tension suppresses the membrane fluctuation and causes the change of free energy.

In the last part, we showed the effects of chemical stimuli, in terms of different chain length and cis position of five monounsaturated fatty acids. Based on their physical properties and our finding results, we can categorize their behaviors in lipid membrane into two types: Oleic acid type which the fatty acid can include in the DPPC region and disturbed the ordered chain length leading to lower in line tension, and Palmitic acid type which can exclude cholesterol from the L_o phase and produce the S_o phase. We also showed their effects under osmotic pressure which can increase line tension in the mixed lipid membranes.

Our findings may provide insight into biophysics of cell membranes how cell response to osmotic pressure without osmotic shock and how unsaturated fatty acids regulate the line tension and can be an insightful model for the understanding of the human cell membrane.

Keywords: osmotic pressure, phase separation, line tension, miscibility temperature, unsaturated fatty acid

Table of contents

Chapter 1 General Introduction……...5

Lipid physiology……6

Lipid membranes.…….10

Raft hypothesis……..13

Phase separation……16

Techniques to study cell membrane……..18

Objectives of this study…….23

Reference…….…..25

Chapter 2 Tension-extended areas of phase separation in phase diagram……...31

Introduction……...32

Materials and Methods……..34

Results……...36

Discussion…….41

Reference……..43

Chapter 3 Tension-induced shift in the miscibility temperature……...46

Introduction……...47

Materials and Methods……..50

Results……...53

Discussion…….58

Reference……..60

Chapter 4 Tension-inhibited domain boundary fluctuation……..63

Introduction.……..64

Materials and Methods……..66

Results……..69
Discussion……....72
Reference……..….77
Chapter 5 Modification of line tension in mixed lipid membranes…….…..84
Introduction…….…..85
Materials and Methods…….….89
Results…….…..94
Discussion……...104
Reference……110
Chapter 6 Summary and conclusion……..114
Acknowledgement…….120
Publication list……...122

Chapter 1 General Introduction

Chapter 1 General Introduction

Lipid physiology

Lipids are a crucial source of energy. It is recommended to take around 20-35% of daily dietary. However, the intake of saturated fatty acids and trans fatty acids should be less than 10% and 2%, respectively. Vegetable sources of lipids are rich in both monounsaturated fatty acids (MUFA) and polyunsaturated fatty acids (PUFA) which provide superior quality than animal lipids. Lipids store in the body as triglycerides constitute. Lipid can be d from the oral cavity by the actions of lingual lipase which secreted by Von Ebner's glands on the dorsal surface of the tongue. It digested around 20-30% of dietary short-chain fatty acids into monoglyceride, diglyceride, and fatty acid, and butyric acid (contains in milk). Lipid can also digest in the stomach by the actions of gastric lipase. The digestion of lipids in the small intestine is performed by bile salts, pancreatic lipase, and intestinal lipase. Bile salts secreted from the liver, are sodium taurocholate and sodium glycocholate in bile. It reduces the interfacial tension and assists the emulsification of fats in the duodenum (Figure 1-1). Pancreatic lipase break ester bond at α-position. Colipase is a coenzyme for lipase. Calcium ions also assist the activity of lipase. Whereas the digestion of cholesterol is acted by cholesterol esterase containing in both pancreatic and intestinal juices (Gupta, 2019). It can hydrolyze cholesterol into triglycerides and cholesteryl ester, and phospholipids. This

activity is also enhanced by bile salts. The phospholipids can be further digested by phospholipase A2 containing in pancreatic juices. The products of this enzyme are fatty acids and lysophospholipids or lysolecithins. The absorption of lipids starts at the lumen of the small intestine. The emulsified products form micelle and diffuse to the brush border of the mucosal cell (Figure 1-2). They enter the cell through the cell membrane and transport to smooth endoplasmic reticulum. Acyl CoA synthase enzyme converts long-chain fatty acids into fatty acyl CoA in the smooth endoplasmic reticulum for the resynthesize of triglyceride, cholesterol ester, and phospholipids in cells. Also, triglycerides, cholesterol ester, phospholipids, and apolipoprotein-A1 and B48 aggregate and form chylomicron inside the smooth endoplasmic reticulum. It sizes around 30 to 60 nm and budded from the Golgi apparatus for exocytosis. Chylomicrons first enter to lacteals and pass through the lymph vessels and thoracic duct. Then these nascent chylomicrons enter the blood circulation called “circulating chylomicrons” (Lopez-Miranda et al., 2007). Lipoprotein lipase locating in blood vessels and capillaries hydrolyze triglyceride in chylomicron and release fatty acids to store in adipose tissues and skeletal muscles. The remaining particles receive apolipoprotein C-II and E are called chylomicron remnants. They were then taken up by very-low-density lipoprotein (VLDL) which export from the liver to delipidating in circulation. Glycerol is absorbed in the lumen of the intestine and passes through the liver by the hepatic portal vein. It will be converted into glycerol-3-phosphate for use in gluconeogenesis pathways (Gupta, 2019). Moreover, living cells can remodeling and modification of

lipids to diverse lipids for their specific functions. Lipids provide so many important functions in living cells including membrane structure components, energy, and heat sources, signaling molecules, protein recruitment platforms, and substrate for post-translational protein-lipid modification. To date, the understanding of how lipids affect biological function is still unclear. Different lipid composition showed different membrane properties and also affect the activity of integral membrane proteins and non-membrane proteins (Harayama & Riezman, 2018). Lipids might regulate come biological processes through membrane properties. Therefore, the study of the physicochemical properties of lipid membranes has attracted much attention currently.

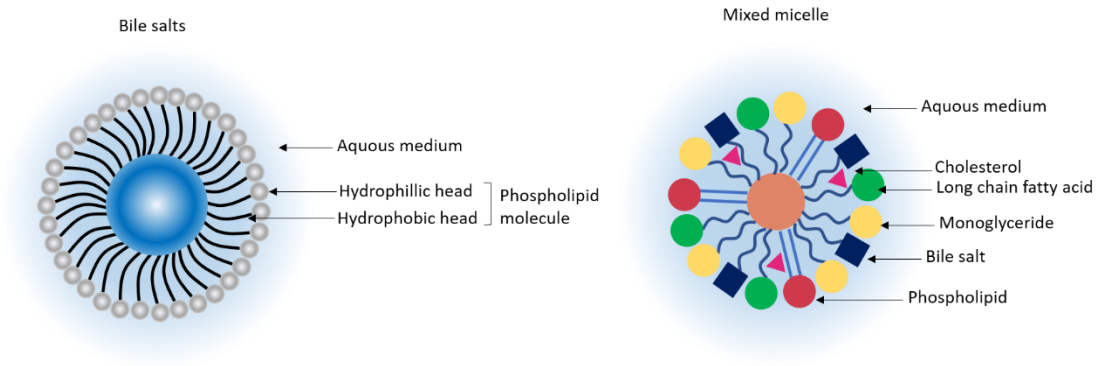

Figure 1-1 Mixed micelle modified from (Gupta, 2019).

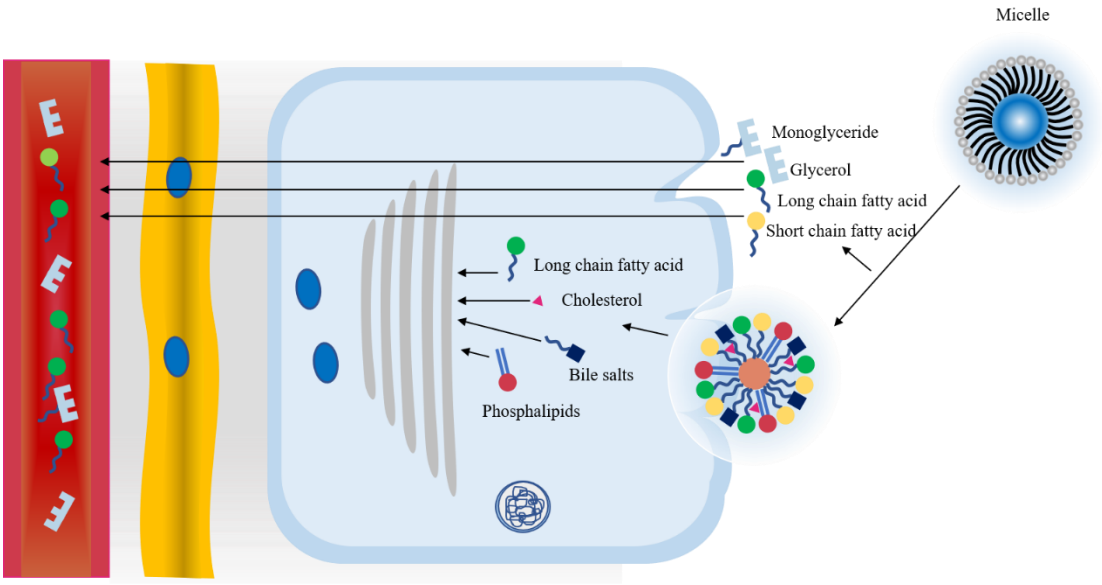

Figure 1-2 Absorption of lipids in enterocyte (Gupta, 2019).

Lipid membrane

Lipids might accomplish their functions by modulating membrane physicochemical properties. There are three major roles of lipids. First, they stored energy as triacylglycerol and stearyl esters elements. Both fatty acid and sterol moieties are essential for membrane biogenesis. Second, the hydrophobic portions are entropically self-associate, and the hydrophilic moieties interact with the aqueous environment, leading to the spontaneous formation of membranes. The nature of the amphiphilic properties of lipids allows cells to separate their internal content from the external environment. The barrier function of the cell enables the membrane to bud, tubulate, split, and coalesce. Third, lipids can act as the first and second messengers in signal transduction (Van Meer et al., 2008). Plasma membrane and endomembrane compartments also response to maintain the organelle structure and function. Eukaryotic cell membranes are formed by several lipid species regarding several functions. Alteration of membrane compositions might lead to pathological conditions of cells (Casares et al., 2019). Phospholipids (PL), glycerophospholipids (GPL), sphingolipids (SL), and cholesterol (Chol) are the common lipid components of the membrane (Figure 1-3). PL, GPL, and SL are categorized by their head group and further classified by their acyl chain length and degree of saturation. This can provide more than 100,000 different species. GPL is the main structural lipids of the eukaryotic cell. They consist of glycerol, two hydrophobic acyl chains, and phosphate moiety which is esterified with choline, serine, ethanolamine, or inositol and turning to the

phosphatidylcholine, phosphatidylserine, phosphatidylethanolamine, and phosphatidylinositol, respectively. The second most abundant lipids in the eukaryotic structure are SL which constructs of one hydrophobic acyl chain and phosphate group linked to the sphingosine backbone. Cholesterol is a vital element of mammalian cell membranes. It contains steroid backbones and a hydroxyl group. The rigidity of steroids and their interaction with SL is the main component of the lipid membrane to resist mechanical stress (Van Meer et al., 2008). The lipid composition of different membranes varies throughout the cell as shown in Figure 1-4. The lipidomic analysis indicated that more than thousands of lipid species are produced to serve the cell membrane for diverse functions including protecting cells from environmental stress (Van Meer, 2005).

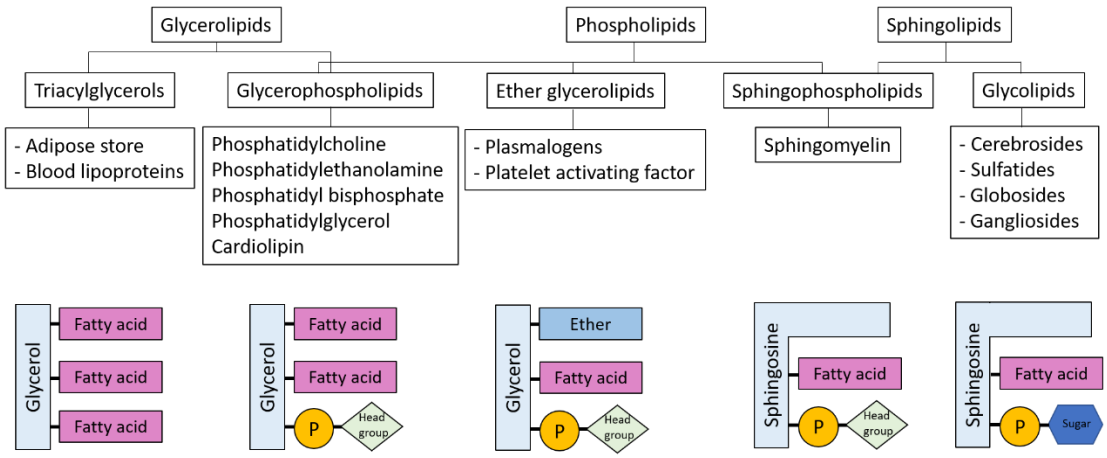

Figure 1-3 Various lipids form in living cell. The picture is modified from (Casares et al., 2019)

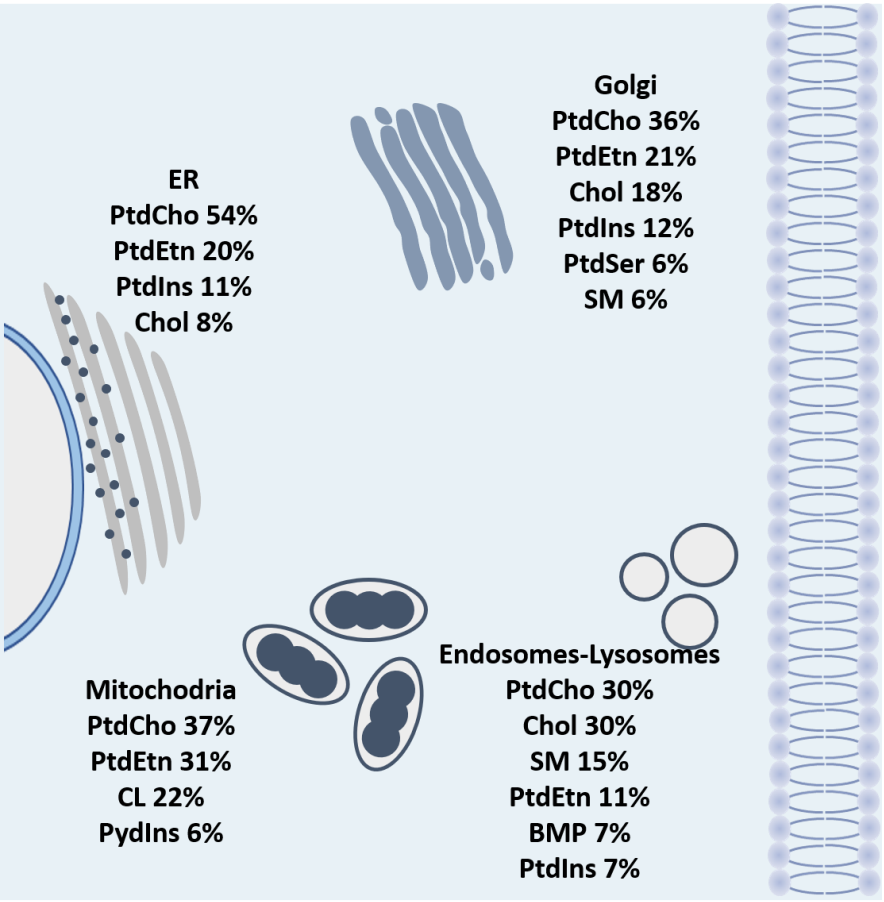

Figure 1-4 Lipids components in organelle. Only lipids containing at least 5% of the totol lipids are shown. BmP: bis(monoacylglycero)phosphate; Chol: cholesterol; CL: cardiolipin; PtdCho: phosphatidylcholine; PtdEtn: phosphatidylethanolamine; PtdIns: phosphatidylinositol; PtdSer: phosphatidylserine; SM:sphingomyelin. Adaped from (Casares et al., 2019)

Raft hypothesis

Cellular plasma membranes are lateral heterogeneous with various compartments and provide different biophysical properties. A year after Singer and Nicolson proposed the fluid mosaic model of cell membrane organization (Singer & Nicolson, 1972). Cell membranes of red blood cells are first observation by separated into detergent-soluble and detergent-resistant fractions (Steck & Yu, 1973). This finding showed that cell membranes are sub-micron scale laterally heterogeneous. The membrane raft hypothesis arose to explain the lateral membrane inhomogeneity, dynamics, and interactions between specific lipids to generate the lateral domains (Raft region) (Sezgin et al., 2017). Raft regions are enriched with cholesterol and saturated phospholipids, sphingolipids, and glycolipids naturally occur of lipids aggregation from the driving of intermolecular interactions (Dietrich et al., 2001). Packing of these hydrophobic compartment domains provides distinctive properties including high order and low fluidity. The nanoscopic domains (10-200 nm) can combine to form the microscopic domains (>300 nm) upon clustering induced by protein-protein, lipid-lipid, and protein-lipid interaction. The presence of some proteins, such as flotillins and caveolins, are particularly found in domain region which is suggested to promote the stability of microdomains (Colin et al., 2016; Lu & Fairn, 2018). Raft regions attracted many by interests from cell biologists, immunologists, and biophysicists since they might associate several vital mechanisms including endocytosis, adhesion, signaling, apoptosis, protein organization, cell homeostasis, and lipid regulation (Veatch & Keller,

2002) (Owen et al., 2012). From the raft hypothesis, the lateral organization of the cell membrane presents discretely as phase separation consisting of the cholesterol-rich rigid domain (rafts, ordered phase, L_o phase) coexisting with the non-raft region or disordered phase (L_d phase). The raft components naturally exist in the living cells in minute size and crosslinked with antibodies or lectins (Simons & Toomre, 2000). However, the visualized of them from the microscope is still limited. The physical properties of the lipid bilayer membrane are widely investigated using the giant unilamellar vesicles (GUVs) as the platforms with various simpler methods including detergent insolubility, single-molecule tracking, fluorescence quenching, fluorescence energy transfer, and aggregation of fluorescently labeled proteins (Veatch & Keller, 2002). Figure 1-5 illustrates the developed tools to study raft membranes.

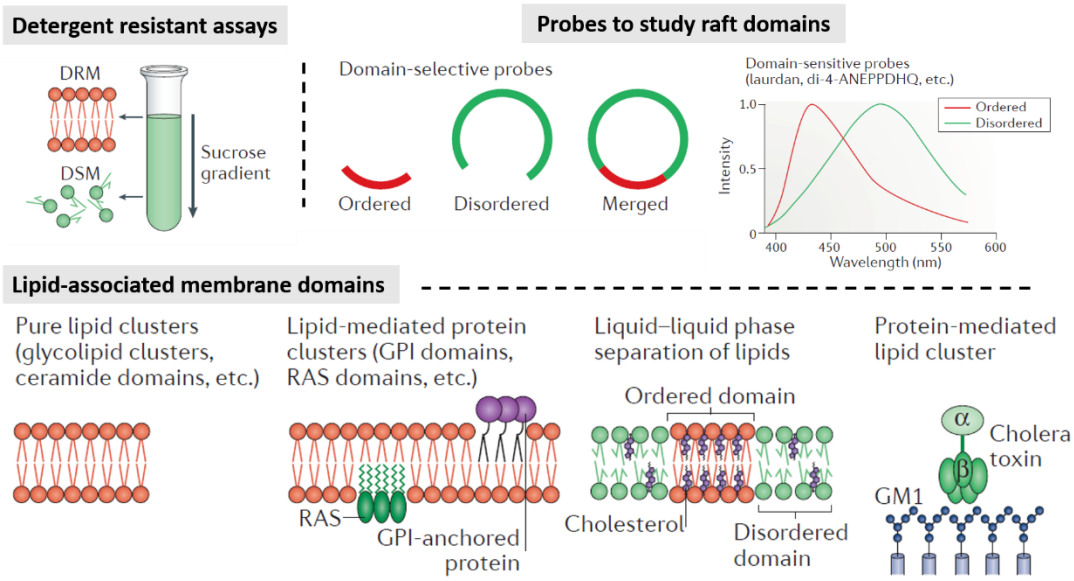

Figure 1-5 Development of lipid rafts studies. Adapted from (Sezgin et al., 2017)

Phase Separation

Phospholipids in water naturally assemble into bilayer structure. Lipid bilayer membrane is the fundamental boundary between inside and outside regions of a cell. It can occur in various phases depending on their structure and environment. These phases have specific properties and functionalities to define the orientation and mobility of membrane lipids and proteins. It was reported that the outer membrane leaflet of human red blood cells is enriched of GPL and sphingomyelin (SM) whereas their inner leaflet is enriched of phosphatidylserine, phosphatidylethanolamine, and phosphatidylinositol. Cholesterol is also an important component of mammalian cells and consists of around 30 mol% of lipids in the cell membrane. The distribution of cholesterol content between the bilayers is still unclear (Devaux & Morris, 2004). Lipid mixtures that mimic those of endoplasmic reticulum are expected to display as the homogeneous liquid-disordered phase at physiological temperatures. However, lipid mixtures that mimic to the outer leaflet of cell membrane display as liquid-ordered (L_o) and liquid-disordered(L_d) domains coexisting in the lateral plane of lipid bilayers (Van Meer et al., 2008). However, in living cell membranes, the domain might exist, but they are too small to observe (<300 nm). The direct visualization of fluorescence microscope cannot be done on the chemically defined artificial membrane model biomembranes of living cells but can observe on the micron-size domain of chemically defined artificial membrane. Combining saturated lipids, unsaturated lipids, and cholesterol in the model membrane results in liquid-liquid phase separation and established two distinct phases.

One is the tighter packing lipids region called liquid-ordered (L_o) phase which is enriched of saturated lipids and cholesterol. Another mobile phase enriched of unsaturated lipids called as liquid-disordered (L_d) phase. The coexistence of solid (S_o) phase and L_d phase are also typically found in the mixture of saturated and unsaturated lipids in low content or without cholesterol content. Indeed, in ternary mixtures of lipid membrane can display one-, two-, and three coexisting phases as shown 2 phase diagrams with different phospholipid pairs (Figure 1-6) (Heberle & Feigenson, 2011). Recently, it was reported that phase-separated membranes can be induced by several factors including lipid compositions, temperature (Veatch & Keller, 2003), chemical substances (Sugahara et al., 2017), adhesion onto the solid substrate (Gordon et al., 2008), and membrane tension (Hamada et al., 2011). Due to the mixing entropy, in higher temperatures, the components in membranes tend to disperse uniformly whereas in lower temperatures the phase separation tends to occur. Phase diagram of a particular mixture of phospholipids, sphingomyelin, and cholesterol also present differently due to the miscibility of the mixing components. Study of such mixtures to determine the extended ratio of domain formation, the phase transition, and lipids interaction at the molecular level which might provide insight into the biophysical properties of biomembranes.

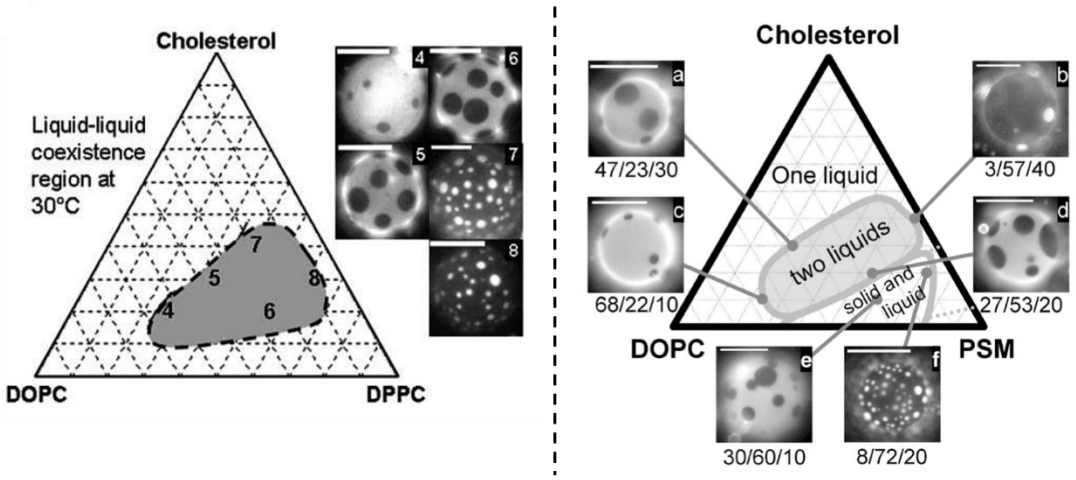

Figure 1-6 Phase diagram of DOPC/DPPC/Chol (left) (Veatch & Keller, 2003) and DOPC/PSM/Chol (Veatch & Keller, 2005)

Flory-Huggins theory

The Flory-Huggins theory is used to explain the phase separation in polymer solution. It was also the common model for phase separation in the lipid membrane. We speculate the phase separation in binary lipid mixtures as the simple model. *N* is defined as the total number of lattice sites, where N_A is the number of lipid A; and N_B *(= N-*N_A*)* is the number of lipid B. $\phi = N_A/N$ is defined as the fraction of lipid A. Then, 1- ϕ is the fraction of lipid B. The entropy can be is expressed by Boltzmann equation

$$S = k_B \ln W.$$

where $\boldsymbol{S}$ is the entropy, $\boldsymbol{k_B}$ is the Boltzmann constant, and W is the number of microstates which is expressed as

$$W = \frac{N!}{N_A!N_B!}.$$

From the sterling formula $\ln M! \simeq M\ln M - M$ $(M \gg 1)$. Therefore, the entropy can be expressed as

$S = k_B\,(N\ln N - N_A\ln N_A - N_B\ln N_B)$

$= k_B\,N(\ln N - \frac{N_A}{N}\ln N_A - \frac{N_B}{N}\ln N_B)$

$= k_B\,N\,(\ln N - \phi\ln N_A - (1-\phi)\ln N_B)$

$= k_B\,N\,[\{\phi + (1-\phi)\}\ln N - \phi\ln N_A - (1-\phi)\ln N_B]$

$= -k_B\,N\,[\,\phi\ln\phi - (1-\phi)\ln(1-\phi)].$

.

From $\boldsymbol{F = U - TS}$, we consequently considered $\boldsymbol{U}$ or the internal interaction between lipids. Only interactions between the adjacent lipids were speculated. $\boldsymbol{\chi_{AA}}$, $\boldsymbol{\chi_{BB}}$, and $\boldsymbol{\chi_{AB}}$ are indicated as the strength of the interactions between lipid A-lipid A, lipid B-lipid B, and lipid A-lipid B, respectively. Therefore, we obtained:

$$U = k_BT\frac{N}{2}[\phi^2\tilde{\chi}_{AA} + (1-\phi)^2\tilde{\chi}_{BB} + 2\phi(1-\phi)\tilde{\chi}_{AB}].$$

where $\tilde{\boldsymbol{\chi}}_{\boldsymbol{mm}} = \boldsymbol{\chi_{mm}/k_BT}$. From $\boldsymbol{F = U - TS}$, the free energy can be obtained as

$$F = k_BT\frac{N}{2}[\phi^2\tilde{\chi}_{AA} + (1-\phi)^2\tilde{\chi}_{BB} + 2\phi(1-\phi)\tilde{\chi}_{AB}] + k_BTN\,[\,\phi\ln\phi - (1-$$

$$\phi) \ln(1-\phi)].$$

To simplify the obtained equation, we defined the mixing free energy as

$$F_{mix}(N,\phi) = F(N,\phi) - F(N\phi,1) - F(N(1-\phi),0).$$

$F(N\phi,1)$ and $F(N(1-\phi),0)$ are the free energy when the system consisting of only lipid A or lipid B, respectively. We can obtain the mixing free energy as

$$F_{mix} = k_B TN\chi\phi(1-\phi) + k_B\, TN\, [\,\phi \ln\phi\, - (1-\phi)\ln(1-\phi)].$$

where $\chi = 2\tilde{\chi}_{AB} - (\tilde{\chi}_{AA} + \tilde{\chi}_{BB})$. The dimensionless mixing free energy per a lipid is denoted as

$$\tilde{f}_{mix} = \chi\phi(1-\phi) + [\,\phi \ln\phi\, - (1-\phi)\ln(1-\phi)].$$

For Flory-Huggins theory, the expression for binodal line which divides homogeneous phase and phase-separated region can be obtained analytically,

$$\chi_b = \frac{1}{2\phi-1} \ln\frac{\phi}{1-\phi}.$$

This is obtained from $\partial\tilde{f}_{mix}/\partial\phi = 0$. Also, the expression for spinodal line which divides unstable and metastable regions can be calculated from $\partial^2\tilde{f}_{mix}/\partial\phi^2 = 0$,

$$\chi_S = \frac{1}{2\phi(1-\phi)}.$$

There are two types of phase separation dynamics: nuclear growth and spinodal decomposition. When the phase transition occurs from homogeneous phase to metastable region, the spinodal decomposition can be observed. Phase-separated two phases are connected each other and bicontinuous structure emerges. As time passes, the width of bicontinuous structure becomes wider and the phase separated region becomes circular due to line tension, and one macro domain is formed finally. On the other hand, for the transition to unstable region, nuclear growth takes place. When domains which become larger than critical size appears, the domains grows up. Domains smaller than critical size is vanished. Such large domains sometimes coalesce each other and one macro domain is also formed as a result. Next part discusses several techniques to study the lipid membrane.

Techniques to study cell membrane

The study of the laterally heterogeneous cell membrane is accomplished from the different solubilization of lipid and proteins membrane by detergent. It was found that the cellular membrane composed of detergent-soluble membrane components (DSMs) and detergent-resistant membrane (DRMs) (Steck & Yu, 1973). DRMs are suggested to enrich of cholesterol, SL, and glycosylphosphatidylinositol (GPI)-anchored proteins (Sezgin et al., 2017). However, this technique might induce phase separation. Besides,

the lipid composition of the cell membrane can be detected by mass spectrometry but samples need to be under high vacuum and freeze-dried (Kraft et al., 2006). Therefore, the artificial model has been developed and used to study the physical aspect behind the raft formation. Due to cell membrane in a living cell is strongly dynamic, disequilibrium, and formation with the vast numbers of different components, using the model system provide the notable advantages to understand the insight of biological membrane from the physical point of view. This model is simple, chemically well-defined, and can be studied in equilibrium conditions. This simplified model can tune the component of liposome from made of a single lipids type or increase the complexity of different lipids types. The model system in which the lipid composition is comparable to the living cell or giant plasma membrane vesicles (GPMVs) can be used to elucidate the basic and common physical aspect of the biological membrane (Alessandrini & Facci, 2014). Whereas the study of different behavior of the model system can provide deeper information on the lipid membrane. Giant unilamellar vesicles (GUVs) which are the unilamellar vesicles with diameter ranged between 10 to 100 μm, have been an important synthetic tool for the biological membrane model. They can be simply prepared by gentle hydration or natural swelling or electroformation technique. Even the observation of cells cannot be resolved by an optical microscope or detected by the confocal microscope, the phase separation of GUVs can be observed under the fluorescence and confocal microscope. The observation requires the contrast agents, fluorescence probes. Several probes have been

developed for lipid rafts research (Klymchenko & Kreder, 2014). Figure 1-8 displays examples of probes partitioning between L_o and L_d phases. Most of the fluorescence probes partition in L_d phases because the highly packed of L_o phases usually exclude the exogenous molecules. The partitioning probes could be divided into two families. The first type is based on fluorescently labeled lipids whereas another one is based on the lipophilic fluorescent molecules. Moreover, atomic force microscopy (AFM) and nuclear magnetic resonance (NMR) were also common techniques for lipid rafts research. AFM can provide the membrane image in nanoscopic resolution. The L_o and L_d phases can be distinguished due to their differences in membranes thickness. Nevertheless, the samples for this technique can be a model membrane or isolated native membranes immobilized on the surface (Alessandrini & Facci, 2014; Tokumasu et al., 2003). NMR can also provide the chemical information of cell membranes such as the head group and acyl chain, but it limits for a simple model membrane (Soni et al., 2008). Figure 1-9 summarizes the common tools for lipid membranes studies.

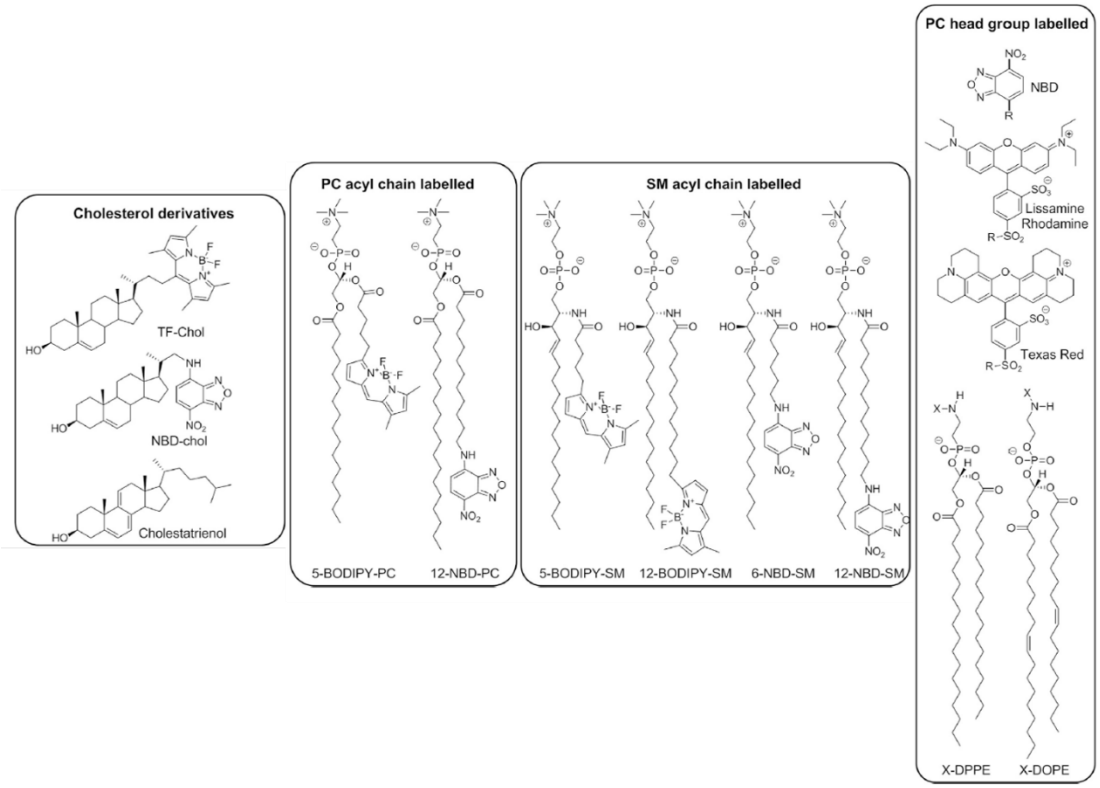

Figure 1-8 Chemical structures of fluorescence lipid derivatives partition between the L_o and L_d phases (Klymchenko & Kreder, 2014).

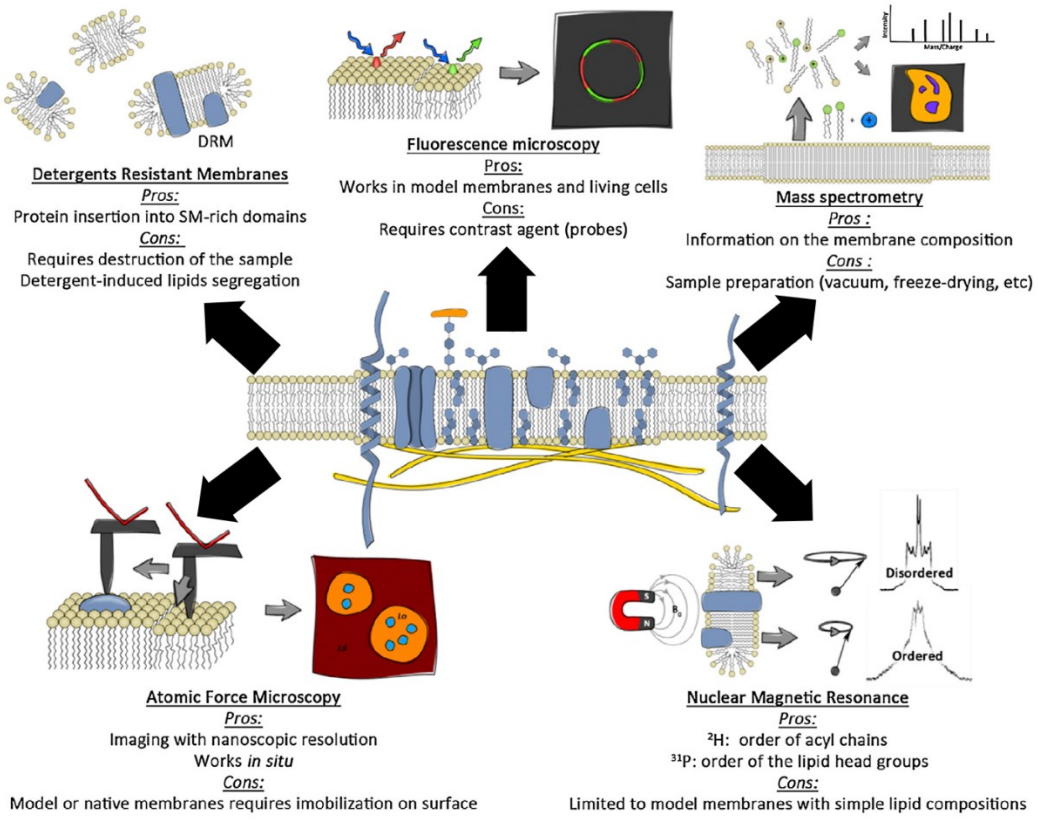

Figure 1-9 Strong and weak points of most common methods used for characterization of lipid rafts (Klymchenko & Kreder, 2014).

Objectives of this study

GUVs have been extensively used as the model to reveal the phase-separated behaviors of a multi-compositional lipid membrane system. Microscope observation on those multi-component lipid vesicles tagging with fluorescence probe can distinguish between saturated lipid and cholesterol-rich phase (L_o phase) and unsaturated lipid-rich phase (L_d phase). Domain formation without cholesterol display a noncircular shape called S_o phase. At higher temperatures, all lipid components are dispersed uniformly due to mixing entropy. A decrease in temperature can induce the phase separation between L_o and L_d phases. This lateral phase separation occurs from the hydrophobic interactions between acyl chains of lipid molecules. Several studies have been fulfilled to reveal the physicochemical properties of biomembranes including study on domain formation (Veatch & Keller, 2005b), domain budding (Baumgart et al., 2003), lipid charge (Himeno et al., 2014), and chemical and physical influence stimuli (Komura et al., 2006; Kubsch et al., 2016). We are interested in how living cells can maintain the homeostasis under stretch or stress including the hemodynamics forces. Also, it has been reported that membrane tension due to the osmotic pressure by the hypotonic solution can change the phase behaviors (Hamada et al., 2011). This study focused on the effects of osmotic pressure, as a physical stimulus, to the phase-separated structures in lipid membranes consisting of DOPC/DPPC/Chol. The application of osmotic pressure was done by placing the lipid vesicles in a hypotonic solution. The phase separation of swollen vesicles was observed by fluorescent microscopy, and the

observation results were summarized in phase diagrams. To discuss the stability of phase-separated domains, miscibility temperature which is the transition temperature between phase separation and homogeneous phase was measured by fluorescent microscopy under precise temperature control. Recently, line tension at the phase-separated domain boundary has received much attention, since it was believed that it is a factor to control the kinetics of phase separation and domain size (Esposito et al., 2007). The height mismatch of acyl chains at the boundary and intermolecular forces contributes to the line tension which is the free energy per unit length of the domain boundary (Stottrup et al., 2019). Therefore, to understand the phase behaviors more precisely, changes of line tension due to osmotic tension were also evaluated based on an analysis of domain boundary fluctuation. In the final part, we also extend the study of line tension under both chemical and physical stimuli. We compared the effects of line tension due to the different length of the acyl chain and cis position of monounsaturated fatty acids, and their effects respond to the osmotic tension. Results might provide insight into a better understanding of the physicochemical properties of cell membranes.

Reference

Alessandrini, A., & Facci, P. (2014). Phase transitions in supported lipid bilayers studied by AFM. *Soft Matter*, *10*(37), 7145–7164. https://doi.org/10.1039/c4sm01104j

Baumgart, T., Hess, S. T., & Webb, W. W. (2003). Imaging coexisting fluid domains in biomembrane models coupling curvature and line tension. *Nature*, *425*(6960), 821–824. https://doi.org/10.1038/nature02013

Casares, D., Escribá, P. V., & Rosselló, C. A. (2019). Membrane lipid composition: Effect on membrane and organelle structure, function and compartmentalization and therapeutic avenues. *International Journal of Molecular Sciences*, *20*(9). https://doi.org/10.3390/ijms20092167

Colin, J., Gregory-Pauron, L., Lanhers, M. C., Claudepierre, T., Corbier, C., Yen, F. T., Malaplate-Armand, C., & Oster, T. (2016). Membrane raft domains and remodeling in aging brain. *Biochimie*, *130*, 178–187. https://doi.org/10.1016/j.biochi.2016.08.014

Devaux, P. F., & Morris, R. (2004). Transmembrane Asymmetry and Lateral Domains in Biological Membranes. *Traffic*, *5*, 241–246. https://doi.org/10.1111/j.1600-0854.2004.00170.x

Dietrich, C., Bagatolli, L. A., Volovyk, Z. N., Thompson, N. L., Levi, M., Jacobson, K., & Gratton, E. (2001). Lipid rafts reconstituted in model membranes. *Biophysical Journal*, *80*(3), 1417–1428. https://doi.org/10.1016/S0006-3495(01)76114-0

Esposito, C., Tian, A., Melamed, S., Johnson, C., Tee, S. Y., & Baumgart, T. (2007). Flicker spectroscopy of thermal lipid bilayer domain boundary fluctuations. *Biophysical Journal*, *93*(9), 3169–3181. https://doi.org/10.1529/biophysj.107.111922

Gordon, V. D., Deserno, M., Andrew, C. M. J., Egelhaaf, S. U., & Poon, W. C. K. (2008). Adhesion promotes phase separation in mixed-lipid membranes. *Epl*, *84*(4). https://doi.org/10.1209/0295-5075/84/48003

Gupta, A. (2019). Comprehensive Biochemistry for Dentistry. *Comprehensivfile:///C:/Users/Nichaporn/Desktop/Dissertation/Ref_forMendeley/Ijms-20-02167 (1).Pdfe Biochemistry for Dentistry*, 441–450. https://doi.org/10.1007/978-981-13-1035-5

Hamada, T., Kishimoto, Y., Nagasaki, T., & Takagi, M. (2011). Lateral phase separation in tense membranes. *Soft Matter*, *7*(19), 9061–9068. https://doi.org/10.1039/c1sm05948c

Harayama, T., & Riezman, H. (2018). Understanding the diversity of membrane lipid

composition. *Nature Reviews Molecular Cell Biology*, *19*(5), 281–296. https://doi.org/10.1038/nrm.2017.138

Heberle, F. A., & Feigenson, G. W. (2011). Phase separation in lipid membranes. *Cold Spring Harbor Perspectives in Biology*, *3*(4), 1–13. https://doi.org/10.1101/cshperspect.a004630

Himeno, H., Shimokawa, N., Komura, S., Andelman, D., Hamada, T., & Takagi, M. (2014). Charge-induced phase separation in lipid membranes. *Soft Matter*, *10*(40), 7959–7967. https://doi.org/10.1039/c4sm01089b

Klymchenko, A. S., & Kreder, R. (2014). Fluorescent probes for lipid rafts: From model membranes to living cells. *Chemistry and Biology*, *21*(1), 97–113. https://doi.org/10.1016/j.chembiol.2013.11.009

Komura, S., Shimokawa, N., & Andelman, D. (2006). Tension-induced morphological transition in mixed lipid bilayers. *Langmuir*, *22*(16), 6771–6774. https://doi.org/10.1021/la053135x

Kraft, M. L., Weber, P. K., Longo, M. L., Hutcheon, I. D., & Boxer, S. G. (2006). Phase separation of lipid membranes analyzed with high-resolution secondary ion mass spectrometry. *Science*, *313*(5795), 1948–1951. https://doi.org/10.1126/science.1130279

Kubsch, B., Robinson, T., Lipowsky, R., & Dimova, R. (2016). Solution Asymmetry

and Salt Expand Fluid-Fluid Coexistence Regions of Charged Membranes. *Biophysical Journal*, *110*(12), 2581–2584. https://doi.org/10.1016/j.bpj.2016.05.028

Lopez-Miranda, J., Williams, C., & Larion, D. (2007). Dietary, physiological, genetic and pathological influences on postprandial lipid metabolism. *British Journal of Nutrition*, *98*(3), 458–473. https://doi.org/10.1017/S000711450774268X

Lu, S. M., & Fairn, G. D. (2018). Mesoscale organization of domains in the plasma membrane–beyond the lipid raft. *Critical Reviews in Biochemistry and Molecular Biology*, *53*(2), 192–207. https://doi.org/10.1080/10409238.2018.1436515

Owen, D. M., Magenau, A., Williamson, D., & Gaus, K. (2012). The lipid raft hypothesis revisited - new insights on raft composition and function from super-resolution fluorescence microscopy. *BioEssays*, *34*(9), 739–747. https://doi.org/10.1002/bies.201200044

Sezgin, E., Levental, I., Mayor, S., & Eggeling, C. (2017). The mystery of membrane organization: Composition, regulation and roles of lipid rafts. *Nature Reviews Molecular Cell Biology*, *18*(6), 361–374. https://doi.org/10.1038/nrm.2017.16

Simons, K., & Toomre, D. (2000). LIPID RAFTS AND SIGNAL TRANSDUCTION. In *NATURE REVIEWS | MOLECULAR CELL BIOLOGY*

(Vol. 1). www.nature.com/reviews/molcellbio

Singer, S. ., & Nicolson, G. L. (1972). Singer1972.Pdf. In *Science* (Vol. 175, pp. 720–731).

Soni, S. P., LoCascio, D. S., Liu, Y., Williams, J. A., Bittman, R., Stillwell, W., & Wassall, S. R. (2008). Docosahexaenoic acid enhances segregation of lipids between raft and nonraft domains: 2H-NMR study. *Biophysical Journal*, *95*(1), 203–214. https://doi.org/10.1529/biophysj.107.123612

Steck, T. L., & Yu, J. (1973). Selective solubilization of proteins from red blood cell membranes by protein perturbants. *Journal of Supramolecular and Cellular Biochemistry*, *1*(3), 220–232. https://doi.org/10.1002/jss.400010307

Stottrup, B. L., Tigrelazo, J., Bagonza, V. B., Kunz, J. C., & Zasadzinski, J. A. (2019). Comparison of Line Tension Measurement Methods for Lipid Monolayers at Liquid-Liquid Coexistence. *Langmuir*, *35*(48), 16053–16061. https://doi.org/10.1021/acs.langmuir.9b01696

Sugahara, K., Shimokawa, N., & Takagi, M. (2017). Thermal stability of phase-separated domains in multicomponent lipid membranes with local anesthetics. *Membranes*, *7*(3). https://doi.org/10.3390/membranes7030033

Tokumasu, F., Jin, A. J., Feigenson, G. W., & Dvorak, J. A. (2003). Nanoscopic lipid domain dynamics revealed by atomic force microscopy. *Biophysical Journal*,

84(4), 2609–2618. https://doi.org/10.1016/S0006-3495(03)75066-8

Van Meer, G. (2005). Cellular lipidomics. *EMBO Journal*, *24*(18), 3159–3165. https://doi.org/10.1038/sj.emboj.7600798

Van Meer, G., Voelker, D. R., & Feigenson, G. W. (2008). Membrane lipids: Where they are and how they behave. *Nature Reviews Molecular Cell Biology*, *9*(2), 112–124. https://doi.org/10.1038/nrm2330

Veatch, S. L., & Keller, S. L. (2002). Organization in Lipid Membranes Containing Cholesterol. *Physical Review Letters*, *89*(26), 1–4. https://doi.org/10.1103/PhysRevLett.89.268101

Veatch, S. L., & Keller, S. L. (2003). Separation of Liquid Phases in Giant Vesicles of Ternary Mixtures of Phospholipids and Cholesterol. *Biophysical Journal*, *85*(5), 3074–3083. https://doi.org/10.1016/S0006-3495(03)74726-2

Veatch, S. L., & Keller, S. L. (2005a). Miscibility phase diagrams of giant vesicles containing sphingomyelin. *Physical Review Letters*, *94*(14), 3–6. https://doi.org/10.1103/PhysRevLett.94.148101

Veatch, S. L., & Keller, S. L. (2005b). Seeing spots: Complex phase behavior in simple membranes. *Biochimica et Biophysica Acta - Molecular Cell Research*, *1746*(3), 172–185. https://doi.org/10.1016/j.bbamcr.2005.06.010

Chapter 2 Tension-extended areas of phase separation in phase diagram

Chapter 2 Tension-extended areas of phase separation in phase diagram

2-1 Introduction

Cell membrane serves as the functional boundary between a cell and its environment, assisting extracellular signal transduction, transporting the nutrients, and homeostasis. To support those extensive functions, membrane organized into lateral domains including the ordered domain (raft) and non-domain regions. The mechanisms of the domain to regulate the biological membrane is still unknown. Recently, several studies focused on the biophysical mechanism of domain formation. Also, it was suggested that lipid can be induced by the changes in physical membrane properties involving membrane thickness, lipid packing density, and surface charge (Sharpe et al., 2010). Several stimuli have been carrying on including the temperature (Veatch et al., 2006), lipid composition (Goh et al., 2013), lipid charge (Himeno et al., 2014), adhesion (Gordon et al., 2008), chemical substances, and hydrostatic pressure (McCarthy et al., 2015). These studies showed that temperature, chemical composition, lipid charge, and adhesion can promote the phase separation to occur. In living cells, in particular, the endothelial cells that lined the blood vessels, it is very interesting to understand that how they react to the hemodynamic forces in form of stretch caused by blood pressure or the shear stress generated by blood flow to maintain homeostasis. It was reported

that the plasma membrane responds differently to stretch and shear stress by rapidly changing lipid order and fluidity in opposite directions (Yamamoto & Ando, 2015). Those behaviors found similarly in both endothelial cells and artificial vesicles consisting of dioleolylphosphocholine (DOPC)/ dipalmitoylphosphocholine (DPPC)/ Cholesterol (Chol). The osmotic swelling is the general characteristic of the bilayer membrane with its semipermeability. It was suggested that osmotic tension can promote large rafts formation (Ayuyan & Cohen, 2006). Also, the oscillatory phase separation is suggested to be induced by the osmotic swelling (Söderlund et al., 2003). Phase behavior of DOPC/DPPC/Chol in a hypotonic solution is qualitatively consistent with that of membranes with tension induced by hypotonic solution (Hamada et al., 2011). Some mixing ratios of DOPC/DPPC/Chol had been examined in that work.

In this chapter, we focused on the response of the lateral organization of lipid membrane to the osmotic tension and extend results to complete the whole phase diagrams in three temperature conditions comparing to the response to osmotic pressure. Results might provide insight into cell homeostasis and survival in several body systems, particularly in the circulation system.

Materials and Methods

Materials

1,2-Dioleoyl-*sn*-glycero-3-phosphocholine (DOPC), 1,2-dipalmitoyl-*sn*-glycero-3-phosphocholine (DPPC), and cholesterol (Chol) were purchased from Avanti Polar Lipids (Alabaster, AL). Rhodamine (Rho)-1,2-dihexadecanoyl-*sn*-glycero-3-phosphoethanol-amine (DHPE) was obtained from Thermo Fisher Scientific (Waltham, US). D(+)-Glucose was purchased from Nacalai Tesque (Kyoto, Japan). Milli-Q water (Specific resistance ≥ 18 MΩ) used in this study was from a Millipore Mill-Q purification system (Burlington, MA).

Vesicles preparation and osmotic tension application

Vesicles were prepared using the natural swelling method. All lipids (0.2 mM) and Rho-DHPE (1 μM) were dissolved in chloroform. The organic solvent was evaporated using nitrogen gas and the formed lipid films are further dried under vacuum for 3 h. To produce the vesicles, films were then pre-heated using 5 μL of Milli-Q water for 10 minutes at 55°C and hydrated using 200 mM of Glucose solution for 3 h at 37°C. The osmotic tension was employed by mixed the vesicle solution with the Milli-Q water at the ratio 1:9 for $\Delta C = 180$. The osmotic pressure is generated due to the difference in glucose concentration between the diluted solution outside and the solution inside.

Microscopic observation

The vesicle solution without osmotic tension and the hypotonic vesicle solution with osmotic tension were comparisons observed under the microscope. They were placed on a glass slide and covered by another coverslip with silicone spacing of *ca.* 0.1 mm. Their percentage of phase behaviors in various lipid compositions ratio were investigated under fluorescence microscopy (Ti-E, Nikon, and IX71, Olympus, Tokyo, Japan). The standard filter sets for detecting Rho fluorescence were Nikon G-2A (ex. 510–560 nm, dichroic mirror 575 nm, em. 580 nm) and Olympus U-MWIG3 (ex. 530–550 nm, dichroic mirror 570 nm, em. 575 nm). The resolution is at 1 pixel = 0.1 μm and 0.16 μm for 100X and 60X objective lens, respectively. The phase behaviors and effects of osmotic tension were studied in three temperature levels: low temperature (10°C), room temperature (24°C), physiological temperature (37°C), and summarized in the phase diagram. The observations were conducted after each sample was incubated at the desired temperature for five minutes using a temperature-controller stage (type 10021, Japan Hitec). Results at each composition were examined from 30 vesicles.

Results

Lateral membrane organization

Various mixtures of DOPC/DPPC/Chol were prepared and investigated at three temperature levels (10°C, 24°C, and 37°C), using a fluorescence microscope. Rhodamine-DHPE was used as a fluorescence probe, which is incorporated into the DOPC-rich region and presents as a bright region. The DPPC-rich region is shown as a dark region. Phase separation is classified as the homogeneous phase, L_o/L_d, and S_o/L_d phase separations (Figure 2-1). Vesicles with a high content of DOPC and cholesterol presented as homogeneous phases as they dispersed uniformly in the lateral membrane. The combination of DOPC and DPPC without cholesterol tends to behave as S_o/L_d phase separation and the membrane becomes more rigid. While including cholesterol in lipid mixture, cholesterol is usually partitioned into the DPPC-rich phase and displayed as L_o/L_d phase separation.

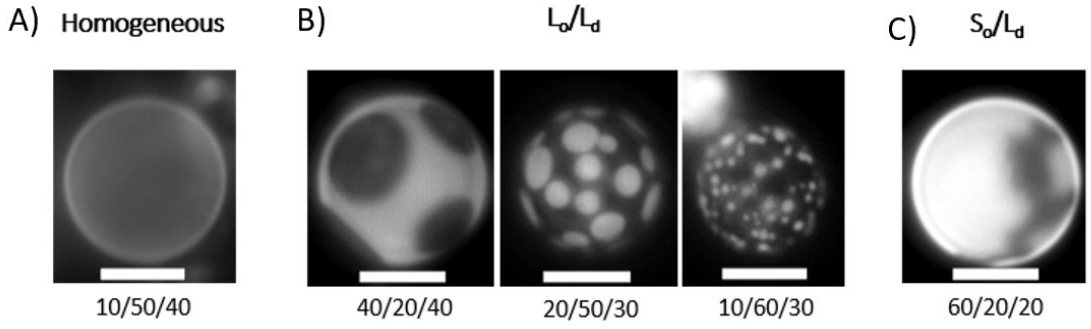

Figure 2-1 Fluorescence microscopic images (scale bar 10 μm).

Results collected from vesicles with 5 to 20 μm and summarized in phase diagrams. Figure 2-2 showed phase diagrams in three temperatures comparing normal and tense membranes. The open, blue, and black circles indicate major populations of the homogeneous phase, L_o/L_d phase separation, and S_o/L_d phase separation, respectively (Figure 2-2). When the number between different populations is very close (±20%), these are classified as the boundary ratios and displayed by two different colors in one circle symbol. At these boundary ratios in the phase diagrams of the homogeneous phase, L_o/L_d, and S_o/L_d phase separation, 50 vesicles were examined to confidently identify the major population. In binary mixtures without cholesterol, only S_o and L_d phases could be produced. As the amount of DPPC increased, it became easier to observe S_o/L_d phase separation. Upon the addition of cholesterol, L_o/L_d was generated. An increase in the amount of cholesterol leads to an increase in cholesterol assembly in the Lo phase (Putzel & Schick, 2008), resulting in the generation of an L_o/L_d phase with greater stiffness (Dolatmoradi et al., 2017). Therefore, the occurring of S_o/L_d phase separation could be more difficult when the amount of cholesterol is increased. Phase separation was found at various ratios, especially at a high fraction of DPPC. However, when the amount of cholesterol was increased to higher than 60%, it was difficult to produce vesicles. When the temperature was set at 10°C, the production of both S_o/L_d and L_o/L_d was increased. However, both S_o/L_d and L_o/L_d were observed only with difficulty when the temperature was increased to 37°C.

Tension-induced phase organization

Tension-induced lateral organization was then investigated. Osmotic pressure was introduced from inside the vesicles by the addition of Milli-Q water to generate a hypotonic solution. The osmotic stress used in this study was set at ΔC = 180 mM, which was reported to highly responsive to phase separation (Hamada et al., 2011), and there was no apparent effect on the survival of vesicles after the application of osmotic stress. The effects of hypotonic stress (ΔC = 180 mM) were studied in ternary systems, at 24°C, 10°C, and 37°C. Vesicles under this hypotonic stress were also confirmed that none rupture presented. Figure 2-2 shows that, with a tensed membrane, the formation of both S_o/L_d and L_o/L_d phase separations is enhanced at all temperature levels. In the phase diagram shown in Figure 2-2(a), at physiological temperature, the membranes tended to be more homogeneous than heterogeneous. When the osmotic stress was increased, these tended to produce domains, as shown by expansion of the phase-separated region toward the high fraction of cholesterol in the phase diagram in Figure. 2-2(d). The states with low DOPC mixing fractions, such as 10/90/0, 20/80/0, 10/80/10, 20/70/10, and 10/60/30, at 10°C without osmotic pressure may show S_o/L_d and/or L_o/L_d phase separation (Figure 2-2c), although we did not observe domains under our experimental conditions. Due to our temperature-controller stages, we used a microscope objective lens of 40X for the observation at 10°C and 100X for 24 and 37°C. With osmotic pressure, we confirmed domains under the same conditions (Figure 2-1f), implying that osmotic pressure made domains larger. Interestingly, the boundary

of the phase separation as shown in Figure 2-2 indicates that the mechanisms of the enhanced phase separation induced by osmotic pressure could be different from those that result from temperature perturbations. A decrease in temperature enlarged the phase separation region toward a high mixing ratio of DOPC, which has a low miscibility temperature. In contrast, the application of osmotic pressure tended to produce phase separation under a high mixing ratio of cholesterol. Notably, we used another saccharide such as sorbitol to confirm the shift of phase separation under osmotic tension. At the typical lipid composition of DOPC/DPPC/Chol = 50/20/30 at room temperature, the application of osmotic tension (ΔC = 180 mM) with sorbitol induced shift of the membrane phase from homogeneous to L_o/L_d phase separation as same as the result with glucose.

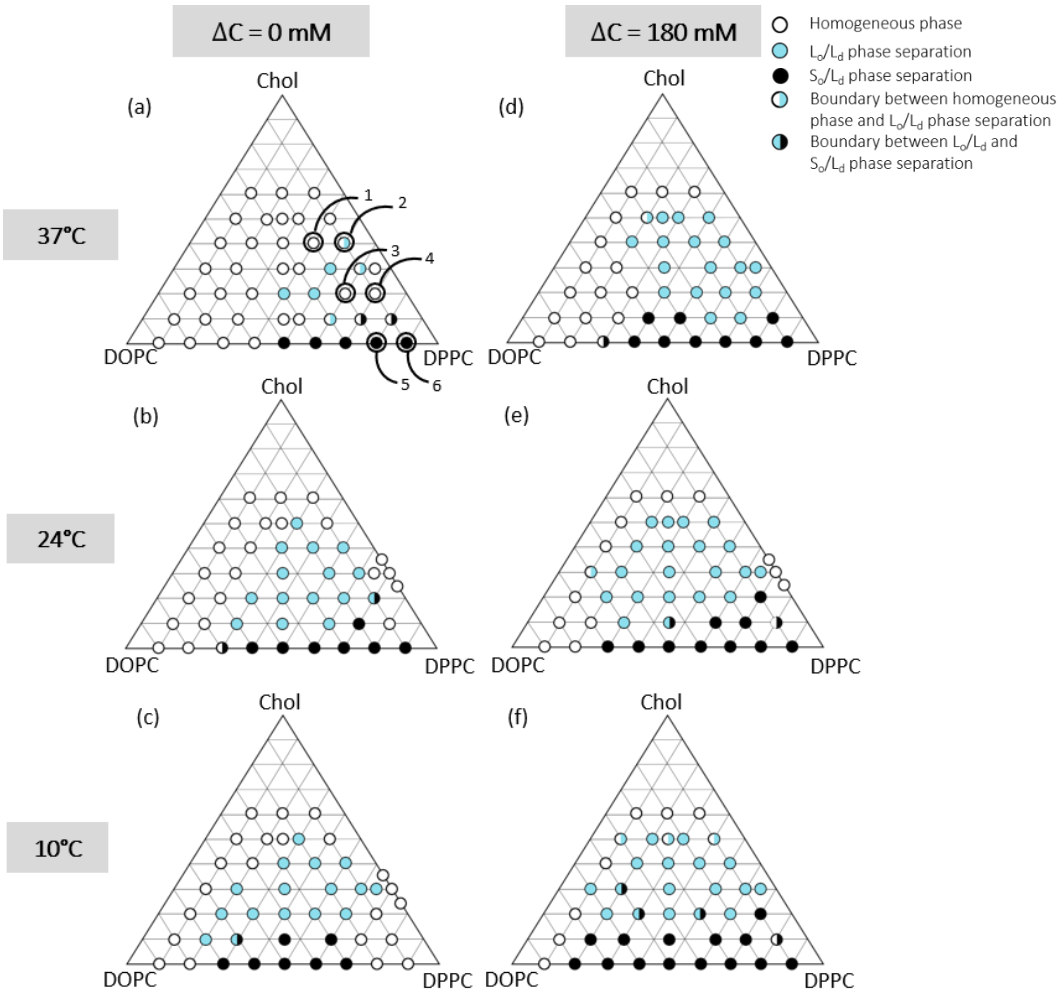

Figure 2-2 Phase diagrams at three temperatures (37°C, 24°C, and 10°C) without/with osmotic tension.

Discussion

The quantitative phase diagram of the phase organization of vesicles at three temperature levels: room temperature, low temperature (10°C), and high temperature (37°C, physiological temperature) have been revealed. Under normal conditions without osmotic pressure, phase separation occurs in systems with various lipid ratios and can be enhanced by decreasing the temperature due to the differences in the miscibility temperature of each lipid (Veatch & Keller, 2002, 2003, 2005). When the temperature is increased above the miscibility temperature, the ordered phase (L_o) transforms into a disordered phase (L_d) (Veatch & Keller, 2003). Therefore, in physiological temperature which is near to the miscibility temperature of DPPC (42°C), the order phase of DPPC transforms into more disorder and distributes together with the DOPC disorder phase. Decrease temperature can enhance the phase separation of the vesicles by the difference lateral lipids organization between the order phase of DPPC and disorder phase of DOPC. Even in a high content of DOPC which is homogeneous in high temperature but the more order chain on DPPC is predominant and shows phase separation. The phase separation can be enhanced even increase the content of DOPC. Additionally, responses to osmotic pressure using glucose hypotonic solution also enhance the phase separation in three temperatures, which is consistent with previous studies (Dolatmoradi et al., 2017; Hamada et al., 2011; Li & Cheng, 2006). Interestingly, the phase diagram results showed that tension-induced phase separation could reflect mechanisms different than those for temperature-induced

phase separation. The increase of tension inside the vesicle causing the water efflux inside the vesicles might lead to reorganizing between the mismatch of the L_o and L_d phase at the lateral organization of the order and disorder phase to reduce the loss of free energy. Phase separation is enhanced with increasing content of DOPC, Chol, and also decreasing temperature. To examine this finding in greater detail, the response of osmotic tension of the miscibility temperature of lipids membranes will be measured in the next chapter.

Reference

Ayuyan, A. G., & Cohen, F. S. (2006). Lipid peroxides promote large rafts: Effects of excitation of probes in fluorescence microscopy and electrochemical reactions during vesicle formation. *Biophysical Journal*, *91*(6), 2172–2183. https://doi.org/10.1529/biophysj.106.087387

Dolatmoradi, A., Mirtaheri, E., & El-Zahab, B. (2017). Thermo-acoustofluidic separation of vesicles based on cholesterol content. *Lab on a Chip*, *17*(7), 1332–1339. https://doi.org/10.1039/c7lc00161d

Goh, S. L., Amazon, J. J., & Feigenson, G. W. (2013). Toward a better raft model: Modulated phases in the four-component bilayer, DSPC/DOPC/POPC/CHOL. *Biophysical Journal*, *104*(4), 853–862. https://doi.org/10.1016/j.bpj.2013.01.003

Gordon, V. D., Deserno, M., Andrew, C. M. J., Egelhaaf, S. U., & Poon, W. C. K. (2008). Adhesion promotes phase separation in mixed-lipid membranes. *Epl*, *84*(4). https://doi.org/10.1209/0295-5075/84/48003

Hamada, T., Kishimoto, Y., Nagasaki, T., & Takagi, M. (2011). Lateral phase separation in tense membranes. *Soft Matter*, *7*(19), 9061–9068. https://doi.org/10.1039/c1sm05948c

Himeno, H., Shimokawa, N., Komura, S., Andelman, D., Hamada, T., & Takagi, M.

(2014). Charge-induced phase separation in lipid membranes. *Soft Matter*, *10*(40), 7959–7967. https://doi.org/10.1039/c4sm01089b

Li, L., & Cheng, J. X. (2006). Coexisting stripe- and patch-shaped domains in giant unilamellar vesicles. *Biochemistry*, *45*(39), 11819–11826. https://doi.org/10.1021/bi060808h

McCarthy, N. L. C., Ces, O., Law, R. V., Seddon, J. M., & Brooks, N. J. (2015). Separation of liquid domains in model membranes induced with high hydrostatic pressure. *Chemical Communications*, *51*(41), 8675–8678. https://doi.org/10.1039/c5cc02134k

Putzel, G. G., & Schick, M. (2008). Phenomenological model and phase behavior of saturated and unsaturated lipids and cholesterol. *Biophysical Journal*, *95*(10), 4756–4762. https://doi.org/10.1529/biophysj.108.136317

Sharpe, H. J., Stevens, T. J., & Munro, S. (2010). A Comprehensive Comparison of Transmembrane Domains Reveals Organelle-Specific Properties. *Cell*, *142*(1), 158–169. https://doi.org/10.1016/j.cell.2010.05.037

Söderlund, T., Alakoskela, J. M. I., Pakkanen, A. L., & Kinnunen, P. K. J. (2003). Comparison of the effects of surface tension and osmotic pressure on the interfacial hydration of a fluid phospholipid bilayer. *Biophysical Journal*, *85*(4), 2333–2341. https://doi.org/10.1016/S0006-3495(03)74657-8

Veatch, S. L., Gawrisch, K., & Keller, S. L. (2006). Closed-loop miscibility gap and quantitative tie-lines in ternary membranes containing diphytanoyl PC. *Biophysical Journal*, *90*(12), 4428–4436. https://doi.org/10.1529/biophysj.105.080283

Veatch, S. L., & Keller, S. L. (2002). Organization in Lipid Membranes Containing Cholesterol. *Physical Review Letters*, *89*(26), 1–4. https://doi.org/10.1103/PhysRevLett.89.268101

Veatch, S. L., & Keller, S. L. (2003). Separation of Liquid Phases in Giant Vesicles of Ternary Mixtures of Phospholipids and Cholesterol. *Biophysical Journal*, *85*(5), 3074–3083. https://doi.org/10.1016/S0006-3495(03)74726-2

Veatch, S. L., & Keller, S. L. (2005). Miscibility phase diagrams of giant vesicles containing sphingomyelin. *Physical Review Letters*, *94*(14), 3–6. https://doi.org/10.1103/PhysRevLett.94.148101

Yamamoto, K., & Ando, J. (2015). Vascular endothelial cell membranes differentiate between stretch and shear stress through transitions in their lipid phases. *American Journal of Physiology - Heart and Circulatory Physiology*, *309*(7), H1178–H1185. https://doi.org/10.1152/ajpheart.00241.2015

Chapter 3 Tension-induced shift in the miscibility temperature

Chapter 3 Tension-induced shift in the miscibility temperature

Introduction

In single component, the transition temperature from solid to liquid phase is called as melting temperature whereas in the multicomponent membrane, the coexistence between S_o/L_d and L_o/L_d phases are defined as mixing temperature or miscibility temperature(T_m) which is normally less than the melting temperature of S_o or L_o phase. T_m corresponds to the boundary temperature between homogeneous and phase-separated vesicles. It is the temperature at which 50% of phase separation occurs. In the ternary component, phase separation occurs when mixing between high melting temperature lipids and low melting temperature lipids. Phase separation occurs when the temperature lower than the transition temperature of lipids in the L_o phase whereas they are completely miscible when the temperature is higher than the transition temperature of lipids in the L_d phase. In general, the transition temperature of pure DOPC and DPPC are -20 °C and 41 °C, respectively. Vesicles with various amounts of lipid components showed diverse T_m values. This means that the interaction between lipids is both temperature- and composition-dependent. It was reported that mixing of C16:0 sphingomyelin with reducing chain length of phosphatidylcholine leads to increasing of T_m. While mixing C16:0 sphingomyelin with a longer chain of phosphatidylcholine results in decreasing of

T_m. This is because T_m of the long chain of phosphatidylcholine is comparable to T_m of sphingomyelin making the interaction between them is less flavor so the T_m is decreased, and vice versa (Térová et al., 2004). T_m does not only relate to the hydrophobic length of lipids molecules but also relate to the interfacial hydrogen bonds between the acyl chains. It was reported that an increase of DOPC and/or sterol contents can suppress T_m (Beattie et al., 2005). The miscibility temperature can be altered by the charge of lipid (Blosser et al., 2013; Himeno et al., 2014). Those study suggested that the attractive interaction between lipid species are significantly stronger than the repulsion interactions between charged headgroups. Therefore, T_m of charge lipids is decrease compared to uncharged lipids. A study of vesicles prepared from negatively charge dioleoylphosphatidylglycerol (DOPG), egg sphingomyelin (eSM), and cholesterol (Chol) in various solutions showed that T_m is lowest in symmetric (in and out) sucrose solution. Interestingly, it increases with the presence of salt and the highest T_m is shown in the symmetric salt system. Results are complementary to the expanded of the L_o/L_d coexistence region in the phase diagram. This implies that salt can stabilize the domain with the increase of DOPG content (Kubsch et al., 2016). T_m of vesicles prepared using 35/35/30 DOPC/DPPC/Chol are shifted differently among a series of alcohol with a various number of carbons due to the partition of alcohol from L_o to L_d phase (Allender & Schick, 2017; Cornell et al., 2017). The local anesthetics (LA) including lidocaine and tetracaine was also reported to lower the thermostability of the L_o phase. Increase content of LA can decrease the T_m since LA might partition in the L_o phase and decrease the thermostability (Sugahara et al., 2017). Moreover, cis- and trans-

conformation of monounsaturated fatty acid affects differently to the DOPC/DPPC/Chol vesicles causing their transition temperature measured by DSC shifts differently. Cis-fatty acid can partition in L_o phase and disturbed the ordered of the L_o phase causing their transition temperature shifts lower whereas trans-fatty acid acts similar to a saturated fatty acid by localized in the L_o phase and excludes cholesterol causing their transition temperature shift higher (Shimokawa et al., 2017). Recently, none of the study reported the effects of miscibility temperature from osmotic tension. Therefore, it is very interesting to compare the effects of tension in the mixed lipid membrane.

Materials and Methods

Materials

1,2-Dioleoyl-*sn*-glycero-3-phosphocholine (DOPC), 1,2-dipalmitoyl-*sn*-glycero-3-phosphocholine (DPPC), and cholesterol (Chol) were purchased from Avanti Polar Lipids (Alabaster, AL). Rhodamine (Rho)-1,2-dihexadecanoyl-*sn*-glycero-3-phosphoethanol-amine (DHPE) was obtained from Thermo Fisher Scientific (Waltham, US). D(+)-Glucose was purchased from Nacalai Tesque (Kyoto, Japan). Milli-Q water (Specific resistance ≥18 MΩ) used in this study was from a Millipore Mill-Q purification system (Burlington, MA).

Vesicles preparation and osmotic tension application

Vesicles were prepared using the natural swelling method. All lipids (0.2 mM) and Rho-DHPE (1 μM) were dissolved in chloroform. The organic solvent was evaporated using nitrogen gas and the formed lipid films are further dried under vacuum for 3 h. To produce the vesicles, films were then pre-heated using 5 μL of Milli-Q water for 10 minutes at 55°C and hydrated using 200 mM of Glucose solution for 3 h at 37°C. The tense vesicles were generated by mixed the vesicle solution with the Milli-Q water at the ratio 1:9 for $\Delta C = 180$.

Microscopic observation

The vesicle solution with and without osmotic tension was placed on a glass slide

and covered by another coverslip with silicone spacing of *ca.* 0.1 mm. Their phase behaviors were investigated under fluorescence microscopy (Ti-E, Nikon, and IX71, Olympus, Tokyo, Japan). The standard filter sets for detecting Rho fluorescence were Nikon G-2A (ex. 510–560 nm, dichroic mirror 575 nm, em. 580 nm) and Olympus U-MWIG3 (ex. 530–550 nm, dichroic mirror 570 nm, em. 575 nm). The resolution is at 1 pixel = 0.1 μm (100X, objective lens). A series of temperature for observation was controlled by a temperature-controller stage (MATS-MORA-BU, TOKAI HIT, Shizuoka, Japan).

Determination of miscibility temperature

The ratio of DOPC/DPPC/Chol 20/40/40, 10/50/40, 20/60/20, 10/70/20, 20/80/0, and 10/90/0 were used for the miscibility temperature analysis. Each composition of tense vesicles was incubated at 40 °C before observation under the microscope. They were quantitatively examined while the temperature was gradually increased from room temperature at intervals of 2 °C using a temperature controller. Thirty vesicles of each composition were counted at each temperature after 5 min incubation on the stage for their equilibrium state. The fractions of phase separation results were examined until the two-phase coexisting region turns to homogeneous vesicles. The resulting data of their phase separation fraction for each composition and each condition were fitted to the Sigmoidal Boltzmann function, as follows:

$$P = \frac{1}{1 + \exp[(T - T_{\mathrm{m}})/dt]} \qquad (1)$$

where P is the fraction of phase-separated vesicle, T_m is the miscibility temperature, and dt is the slope of sigmoidal curve. The miscibility temperature is the boundary between one- and two-phase regions. It is defined as the temperature at which 50% of phase separation occurs. Results were summarized as chart.

Results

Tension-induced membranes shift the miscibility temperature

Responses of miscibility temperature to hypotonic stress were also examined in lipids mixtures with different cholesterol (0%, 20%, 40%). Percentage of phase-separated vesicles were collected from (1) 20/40/40; (2) 10/50/40; (3) 20/60/20; (4) 10/70/20; (5) 20/80/0; and (6) 10/90/0 among different temperature (Figure 2-2(a)). The phase-separated fractions were collected from room temperature and a series of escalated temperature with 2°C intervals. Those resulting data were fitted to equation 1. In the presence of cholesterol, the S_o phase turns to the L_o phase. The miscibility temperature and the response of osmotic stress of (1) 20/40/40; (2) 10/50/40; (3) 20/60/20; (4) 10/70/20; (5) 20/80/0; and (6) 10/90/0 were shown in Table 3-1. Figure 3-1 obviously showed the shift of miscibility temperature due to the osmotic tension, and the bright and dark regions correspond to L_o and L_d phase separation. The response of hypotonic tress showed the shifted of miscibility temperature which agrees of the extended area of phase separation in the phase diagram (Figure 2-2). Interestingly, it was found that the miscibility temperature increased greatly at higher cholesterol concentrations. The average miscibility temperature shifts of L_o/L_d (DOPC/DPPC/Chol =20/40/40, 10/50/40, and 20/60/20) and S_o/L_d (DOPC/DPPC/Chol =10/70/20, 20/80/0, and 10/90/0) were 13.6 °C and 2.5 °C, respectively. Smodyrev et al. reported that cholesterol and DPPC are packed more densely than DPPC alone. The interaction of cholesterol in the L_o phase may

play a role in enhancing phase separation by shifting the transition temperature.

Table 3-1 Miscibility temperature with different cholesterol (0%, 20%, 40%) in lipids mixtures membrane and tense-membrane

Ratio	DOPC/DPPC/Chol	T_m (°C)	
		$\Delta C = 0$	$\Delta C = 180$
1	20/40/40	31.9	44.9
2	10/50/40	34.1	50.8
3	20/60/20	27.8	38.8
4	10/70/20	37.3	40.2
5	20/80/0	42.2	44.5
6	10/90/0	42.9	45.2

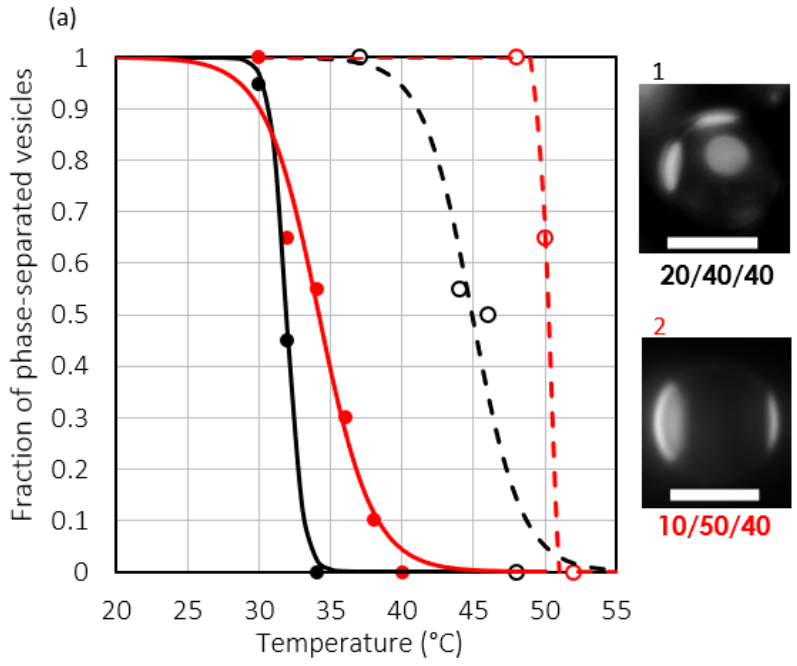
(a)
Fraction of phase-separated vesicles
1
0.9
0.8
0.7
0.6
0.5
0.4
0.3
0.2
0.1
0
20
25
30
35
40
45
50
55
Temperature (°C)
1
20/40/40
2
10/50/40

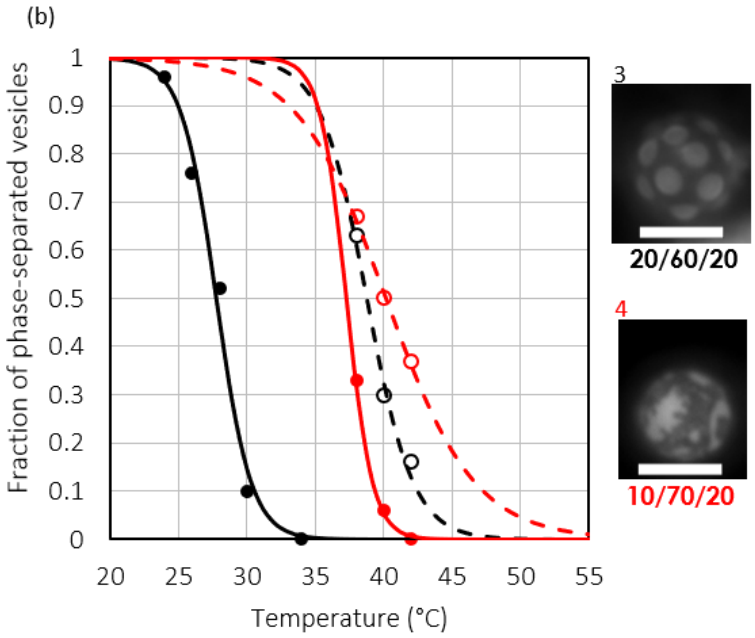
(b)
Fraction of phase-separated vesicles
1
0.9
0.8
0.7
0.6
0.5
0.4
0.3
0.2
0.1
0
20
25
30
35
40
45
50
55
Temperature (°C)
3
20/60/20
4
10/70/20

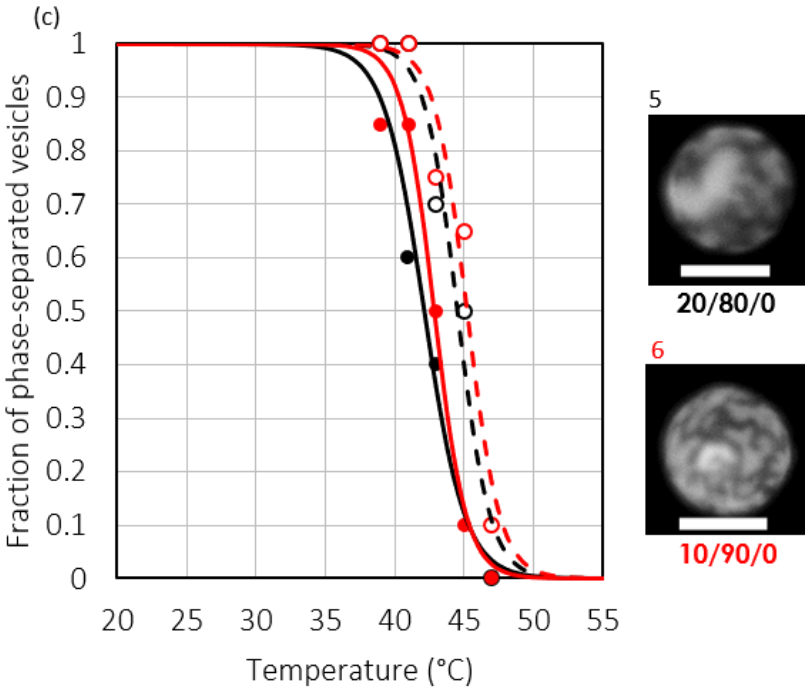

Figure 3-1 Tension-shifted miscibility temperatures were obtained at 40% cholesterol (a), 20% cholesterol (b), and 0% cholesterol (c). Microscopic images were observed at room temperature: (a1) 20/40/40 defined as DOPC 20%, DPPC 40%, and Chol 40%, (a2) 10/50/40 defined as DOPC 10%, DPPC 50%, and Chol 40%, (b3) 20/60/20 defined as DOPC 20%, DPPC 60%, and Chol 20%, (b4) 10/70/20 defined as DOPC 10%, DPPC 70%, and Chol 20%, (c5) 20/80/0 defined as DOPC 20%, DPPC 80%, and Chol 0%, (c6) 10/90/0 defined as DOPC 10%, DPPC 90%, and Chol 0%. These compositions correspond to those in Fig. 1a 1-6. Solid and dashed lines represent the fraction of phase-separated vesicles without and with osmotic tension, respectively. The lines were obtained by fitting the experimental data (filled circle without osmotic tension and open circle with osmotic tension) with the Sigmoidal Boltzmann function of eq. (1). Black and red color represented as fraction of DOPC 20% and 10%, respectively. Scale bars in the microscopic images are 10 μm.

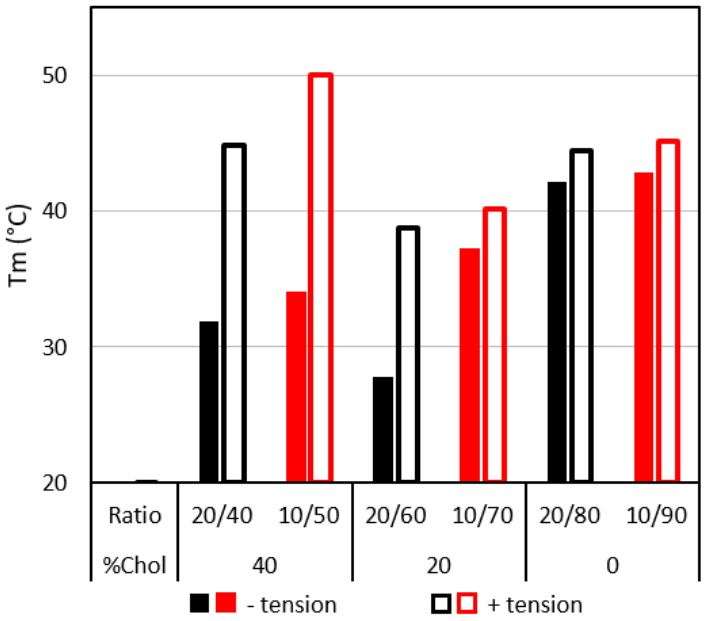

Figure 3-2 Shift in the miscibility temperature according to the Chol concentration. The x-axis shows the ratio of DOPC/DPPC. Closed and open bars indicate results without and with osmotic tension, respectively.

Discussion

The miscibility temperature results showed that an increase in cholesterol content tends to decrease the miscibility temperature. Results are in agreement with previous studies (Beattie et al., 2005; Redondo-Morata et al., 2012; Veatch & Keller, 2002). This might be a consequence of the localization of cholesterol is commonly incorporated into the L_o phase more than the L_d phase. Also, the packed of cholesterol and DPPC are more densely than DPPC alone (Davis et al., 2009; Smondyrev & Berkowitz, 1999). The more fluidity of the L_o phase is possibly repressing the miscibility temperature of the order phase (high-melting temperature lipid-rich phase) to be lower and determines the miscible of the coexisting between L_o and L_d phases to be lower, as well. Whereas at the constant content of cholesterol, an increase of DPPC content enhances the increase of T_m. Interestingly, the responsiveness of membrane in hypotonic swelling (ΔC = 180 mM) showed the shifted in the miscibility temperature. Moreover, results showed that the miscibility temperature of the 40% cholesterol-containing vesicle exhibited a larger shift due to tension-induced perturbation than that of its 20% cholesterol-containing counterpart. Therefore, response to osmotic pressure in the L_o phase (with cholesterol) was much higher than that in the S_o phase. Differences response between L_o and S_o phases also found in the response of them to the local anesthetics (Sugahara et al., 2017). This might be the effect of the localization of cholesterol in the order phase (L_o) can increase the fluidity of the order phase (Takechi-Haraya et al., 2016). Therefore, the more fluidity vesicles are possible higher responsive for the hypotonic swelling that the more rigidity vesicles. In addition, the interaction of

cholesterol in the Lo phase may play a role in enhancing phase separation by shifting the transition temperature. Future interest in the line tension analysis is explained in the next chapter.

Reference

Allender, D. W., & Schick, M. (2017). The Effect of Solutes on the Temperature of Miscibility Transitions in Multicomponent Membranes. *Biophysical Journal*, *113*(8), 1814–1821. https://doi.org/10.1016/j.bpj.2017.08.033

Beattie, M. E., Veatch, S. L., Stottrup, B. L., & Keller, S. L. (2005). Sterol structure determines miscibility versus melting transitions in lipid vesicles. *Biophysical Journal*, *89*(3), 1760–1768. https://doi.org/10.1529/biophysj.104.049635

Blosser, M. C., Starr, J. B., Turtle, C. W., Ashcraft, J., & Keller, S. L. (2013). Minimal effect of lipid charge on membrane miscibility phase behavior in three ternary systems. *Biophysical Journal*, *104*(12), 2629–2638. https://doi.org/10.1016/j.bpj.2013.04.055

Cornell, C. E., McCarthy, N. L. C., Levental, K. R., Levental, I., Brooks, N. J., & Keller, S. L. (2017). n-Alcohol Length Governs Shift in Lo-Ld Mixing Temperatures in Synthetic and Cell-Derived Membranes. *Biophysical Journal*, *113*(6), 1200–1211. https://doi.org/10.1016/j.bpj.2017.06.066

Davis, J. H., Clair, J. J., & Juhasz, J. (2009). Phase equilibria in DOPC/DPPC-d62/cholesterol mixtures. *Biophysical Journal*, *96*(2), 521–539. https://doi.org/10.1016/j.bpj.2008.09.042

Himeno, H., Shimokawa, N., Komura, S., Andelman, D., Hamada, T., & Takagi,

M. (2014). Charge-induced phase separation in lipid membranes. *Soft Matter*, *10*(40), 7959–7967. https://doi.org/10.1039/c4sm01089b

Kubsch, B., Robinson, T., Lipowsky, R., & Dimova, R. (2016). Solution Asymmetry and Salt Expand Fluid-Fluid Coexistence Regions of Charged Membranes. *Biophysical Journal*, *110*(12), 2581–2584. https://doi.org/10.1016/j.bpj.2016.05.028

Redondo-Morata, L., Giannotti, M. I., & Sanz, F. (2012). Influence of cholesterol on the phase transition of lipid bilayers: A temperature-controlled force spectroscopy study. *Langmuir*, *28*(35), 12851–12860. https://doi.org/10.1021/la302620t

Shimokawa, N., Mukai, R., Nagata, M., & Takagi, M. (2017). Formation of modulated phases and domain rigidification in fatty acid-containing lipid membranes. *Physical Chemistry Chemical Physics*, *19*(20), 13252–13263. https://doi.org/10.1039/c7cp01201b

Smondyrev, A. M., & Berkowitz, M. L. (1999). Structure of dipalmitoylphosphatidylcholine/cholesterol bilayer at low and high cholesterol concentrations: Molecular dynamics simulation. *Biophysical Journal*, *77*(4), 2075–2089. https://doi.org/10.1016/S0006-3495(99)77049-9

Sugahara, K., Shimokawa, N., & Takagi, M. (2017). Thermal stability of phase-separated domains in multicomponent lipid membranes with local anesthetics. *Membranes*, *7*(3). https://doi.org/10.3390/membranes7030033

Takechi-Haraya, Y., Sakai-Kato, K., Abe, Y., Kawanishi, T., Okuda, H., & Goda, Y. (2016). Atomic Force Microscopic Analysis of the Effect of Lipid Composition on Liposome Membrane Rigidity. *Langmuir*, *32*(24), 6074–6082. https://doi.org/10.1021/acs.langmuir.6b00741

Térová, B., Peter Slotte, J., & Nyholm, T. K. M. (2004). Miscibility of acyl-chain defined phosphatidylcholines with N-palmitoyl sphingomyelin in bilayer membranes. *Biochimica et Biophysica Acta - Biomembranes*, *1667*(2), 182–189. https://doi.org/10.1016/j.bbamem.2004.10.003

Veatch, S. L., & Keller, S. L. (2002). Organization in Lipid Membranes Containing Cholesterol. *Physical Review Letters*, *89*(26), 1–4. https://doi.org/10.1103/PhysRevLett.89.268101

Chapter 4 Tension-inhibited domain boundary fluctuation

Chapter 4 Tension-inhibited domain boundary fluctuation

Introduction

In the biomembranes model, the raft domains can be observed under fluorescence microscopy. These domains are enriched with high melting temperature lipids (saturated lipids) and cholesterol and appear as L_o phase. It coexists with a L_d phase which is enriched with low melting temperature (unsaturated lipids). The domain exhibits in a circular shape. The inclination to minimize the boundary length indicates the presence of line tension at the phase interface. The difference of thickness between L_o (thicker) and L_d phase causing the height mismatch at the domain edge. The hydrophobic of the acyl chain is an unfavorable energetic effect against the aqueous solution leading to the membrane distort. Line tension (λ) is the free energy-carrying in the height mismatch per unit of length of the domain boundary. Line tension is believed to be the main factor to determine the size of the domain together with other factors including the total boundary length, entropy, and electrostatic repulsion (Kuzmin et al., 2005). It was suggested that increase hydrophobic height mismatch can increase line tension and miscibility temperature and lead to enlargement of the domain size (García-Sáez et al., 2007). A recent study clearly showed that line tension determines the size of the domain in lipid components mimic cell membranes systems. The first micron-scale domain appeared at a line tension of 0.3 pN (Usery et al., 2017).

Moreover, line tension is temperature-dependent. It decreases when the temperature increases close to the miscibility temperature. Interestingly, the decrease of line tension is linear to zero at the miscibility temperature (Honerkamp-Smith et al., 2008). Differences in lipid composition, chain length, chain tilt, dipole density also govern the magnitude of line tension (Lee et al., 2011). It was suggested that increase DOPC content can increase the line tension whereas increase of cholesterol content can reduce line tension (Tsai & Feigenson, 2019). Also, some physical stimuli including the hydrostatic force, membrane adherence onto solid substrate, and tension can alter the line tension as domain boundary (Gordon et al., 2008; Portet et al., 2012). Line tension could, therefore, be an important parameter to regulate several functions of biological membranes. The established domain boundary flicker spectroscopy is the promising technique used for measure line tension and results from this technique are consistent with the theoretical critical exponent (Esposito et al., 2007; Stottrup et al., 2019). Recently, none of the studies examine the effects of osmotic swelling on the line tension of membrane domains. In this study, changes in line tension due to osmotic pressure were evaluated based on an analysis of domain boundary fluctuation.

Materials and Methods

Materials

1,2-Dioleoyl-*sn*-glycero-3-phosphocholine (DOPC), 1,2-dipalmitoyl-*sn*-glycero-3-phosphocholine (DPPC), 1,2-diphytanoyl-*sn*-glycero-3-phosphocholine (DiphyPC) and cholesterol (Chol) were purchased from Avanti Polar Lipids (Alabaster, AL). Rhodamine (Rho)-1,2-dihexadecanoyl-*sn*-glycero-3-phosphoethanol-amine (DHPE) was obtained from Thermo Fisher Scientific (Waltham, US). D(+)-Glucose was purchased from Nacalai Tesque (Kyoto, Japan). Milli-Q water (Specific resistance ≥18 MΩ) used in this study was from a Millipore Mill-Q purification system (Burlington, MA).

Vesicles preparation and osmotic tension application

Vesicles were prepared using the natural swelling method. All lipids (0.2 mM) and Rho-DHPE (1 μM) were dissolved in chloroform. The organic solvent was evaporated using nitrogen gas and the formed lipid films are further dried under vacuum for 3 h. To produce the vesicles, films were then pre-heated using 5 μL of Milli-Q water for 10 minutes at 55°C and hydrated using 200 mM of Glucose solution for 3 h at 37°C. The tense vesicles were produced by mixed the vesicle solution with the Milli-Q water at the ratio 1:9 for $\Delta C = 180$.

Microscopic observation

Samples were placed on a glass slide and covered by another coverslip with silicone spacing of *ca.* 0.1 mm. Their phase behaviors were investigated under fluorescence microscopy (Ti-E, Nikon, and IX71, Olympus, Tokyo, Japan). The standard filter sets for detecting Rho fluorescence were Nikon G-2A (ex. 510–560 nm, dichroic mirror 575 nm, em. 580 nm) and Olympus U-MWIG3 (ex. 530–550 nm, dichroic mirror 570 nm, em. 575 nm). The resolution is at 1 pixel = 0.1 μm for 100X objective lens. All samples were observed at room temperature.

Flicker spectroscopy of domain boundary fluctuation

Line tension at the domain boundary fluctuation was measured from a movie of >1 sec (at 30 frames per second) of a phase-separated domain. The radius of the domain was traced along the perimeters of binary images using ImageJ software. Line tension results at domain boundary fluctuation were then calculated using in-house software by plotted the domain radius (r) as the function of the polar angle (ψ) (Stottrup et al., 2019). The fluctuating domain boundary was presented in terms of a Fourier series expansion:

$$r(\psi) = r_{\mathrm{av}}\left[1 + a_o + \sum_{k=1}^{\infty} a_k \cos(k\psi) + \sum_{k=1}^{\infty} b_k \sin(k\psi)\right] \qquad (2)$$

where $\boldsymbol{r_{av}}$ is the average domain radius, $\boldsymbol{k}$ is the mode number, and $\boldsymbol{a_k}$ and $\boldsymbol{b_k}$ are Fourier coefficients. The fluctuation and the excess free energy is expressed as

$$\Delta F \simeq \frac{\pi r_{\mathrm{av}}}{2}\gamma \sum_{k=2}^{\infty}(k^2-1)\,(a_k^2+b_k^2) \qquad (3)$$

where $\boldsymbol{\gamma}$ is the line tension. The free energy for each independent mode is $\boldsymbol{k_B T}$ from the generalized equipartition theorem. Therefore, we obtain:

$$\langle a_k^2\rangle + \langle b_k^2\rangle = \frac{2k_{\mathrm{B}}T}{\pi r_{\mathrm{av}}\gamma}\left(\frac{1}{k^2-1}\right) \qquad (4)$$

where $\langle \ldots \rangle$ is the average value of all images. The line tension $\boldsymbol{\gamma}$ can be obtained by applying linear regression to the relationship of the mode number $\boldsymbol{k}$ and the Fourier coefficients $\boldsymbol{a_k}$ and $\boldsymbol{b_k}$, as described by equation (4).

Results

Tension-induced membrane influence line tension

Line tension at a domain boundary is another factor that affects the stability of membrane phase formation. It is therefore interesting to study the line tension influenced by osmotic swelling. DiphyPC (diphytanoyl-phosphatidylcholine), a branched saturated lipid, was used to compare the line tension with the DOPC system since domains produced by this type of lipid showed clear fluctuation (Honerkamp-Smith et al., 2008; Veatch et al., 2006). Figure 4-1(a) shows the images of fluctuated domains and Fig. 4-1(b) indicates the domain radius parametrized, in terms of radians (Θ). The line tension was calculated by a domain fluctuation analysis from several images that showed the isolated domain at the center of the vesicle. The domain boundary fluctuation of five to ten vesicles was recorded for more than 1 sec (30 frames) for both DOPC/DPPC/Chol 20/40/40 and DiphyPC/DPPC/Chol 25/35/45 at room temperature. The radius of the domains was traced and analyzed using ImageJ software, and the line tension values were calculated using Eqs. 2 to 4. The Fourier amplitude of the edge fluctuation corresponding to Fig. 4-1(b) as a function of wavenumber (k) as shown in Fig. 4-1(c). The linear fit of experimental data with Eq. 4 gives us the line tension (Fig. 4-1(d)). The results showed that osmotic stress can enhance the line tension from 0.4±0.3 to 1.2±1.2 pN in the DiphyPC system and from 0.6±0.3 to 1.8±0.5 pN in the DOPC system, at room temperature.

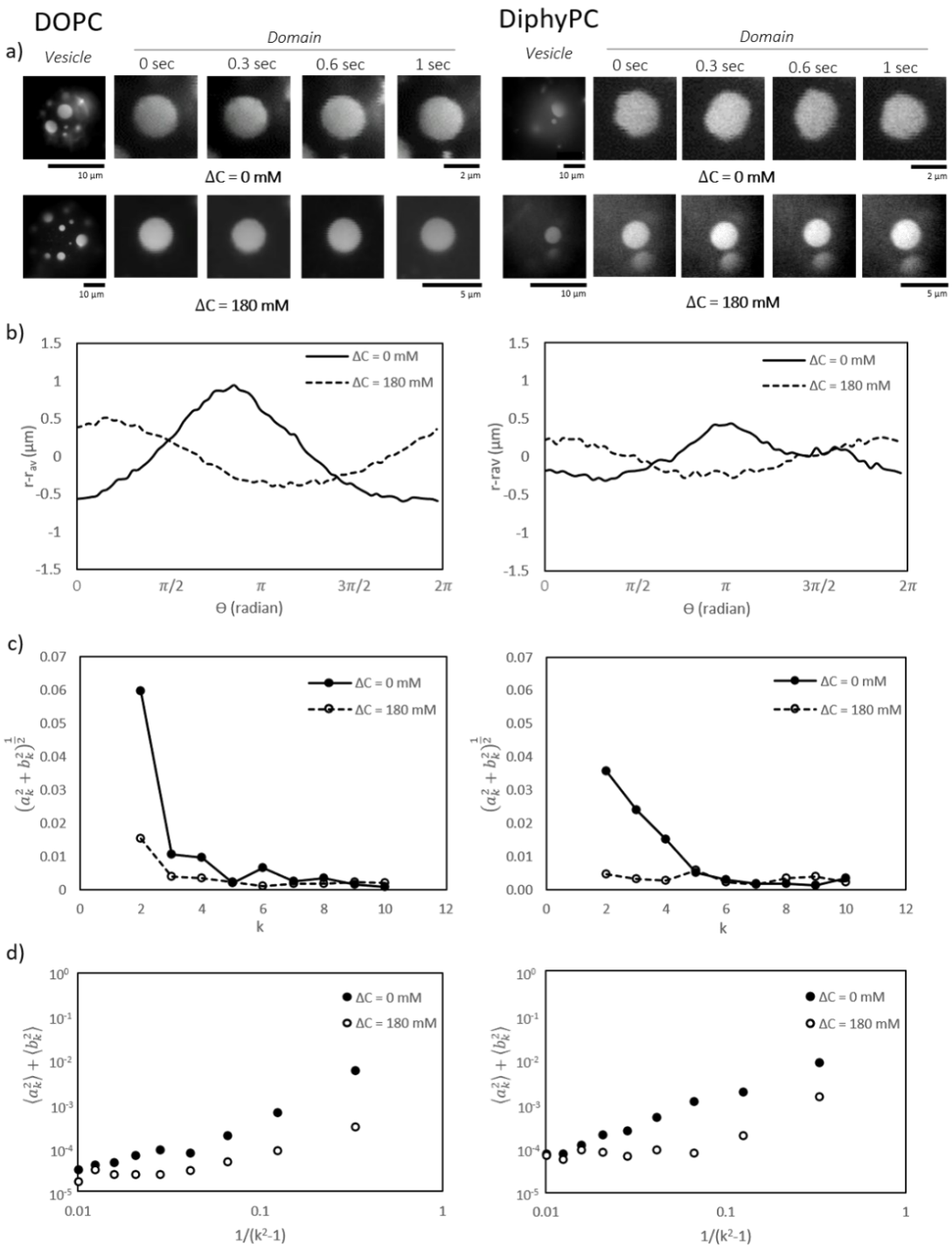

Figure 4-1 a) Domain boundary fluctuation for DOPC/DPPC/Chol=20/40/40 (Top left)

and DiphyPC/DPPC/Chol=25/35/40 (Top right). Microscopic images were observed at room temperature. b) Radial fluctuation as a function of polar angle Θ. Average domain radius (r_{av}) of DOPC with ΔC = 0 mM and ΔC = 180 mM are 1.49 and 2.26 mm, whereas those of DiphyPC system with ΔC = 0 mM and ΔC = 180 mM are 1.48 and 2.04 mm. c) Amplitude $[(a_k^2 + b_k^2)^{\frac{1}{2}}]$ versus wavenumber (k) of the edge fluctuation, as obtained by Eq. (2). d) Double-logarithmic plot of Fourier coefficients against $1/(k^2-1)$.

Discussion

The response of the domain boundary fluctuation to the osmotic pressure of the DOPC system was suppressed, corresponding to the results with the DiphyPC system. Although DOPC and DiphyPC have low chain melting temperatures, the structure of the acyl chain is different: DOPC has a double bond and DiphyPC is branched. Osmotic stress affected the phase behavior of both lipid systems. The phase separation was enhanced due to the suppression of domain boundary fluctuation, as shown by our results that line tension increased with an increase in osmotic pressure. We consider the possible mechanism of osmotic swelling-induced phase separation. An increase membrane tension by the adhesion of membranes was reported to suppress undulation to produce phase separation (Gordon et al., 2008). The osmotic swelling in our experiments also induced membrane tension. In term of free energy of the membrane, the degree of membrane undulation is inversely proportional to the rigidity of the membrane as $\sim\frac{\boldsymbol{k_B T}}{\boldsymbol{\kappa q^4}}$, where κ is the bending rigidity of the membrane and $\boldsymbol{q}$ is the wave vector of the undulation mode (Hed & Safran, 2003). Due to membrane stiffness, L_d phase membranes show greater undulation than L_o and S_o phase membranes. When the undulation is suppressed under tension, to avoid the reduction of undulation entropy, homogeneous vesicles tend to phase-separate into L_o/L_d or S_o/L_d. The free energy of phase separation (energy difference between phase separation and homogeneous states: $\Delta \boldsymbol{f} = \boldsymbol{f}^{\text{phase separation}} - \boldsymbol{f}^{\text{homogeneous}}$) is expressed as:

$$\Delta \boldsymbol{f} = \boldsymbol{f}_{\mathbf{mix}} + \boldsymbol{f}_{\mathbf{und}}, \qquad (5)$$

where the first term is a classical mixing free energy and the second term is an undulation contribution. We assume that the mixing term does not change under osmotic tension and focus on the undulation term. Gordon et al. showed that undulation term was expressed as (Gordon et al., 2015):

$$\boldsymbol{f}_{\mathbf{und}} = \frac{\pi k_{\mathrm{B}} T}{4a^2} \ln \frac{\kappa_{\mathrm{A}} \kappa_{\mathrm{B}}}{\kappa_{\mathrm{AB}}^2}, \qquad (6)$$

where $\boldsymbol{a} = \boldsymbol{2\pi/q_{>}}$ is the smallest cut-off length for a continuum description, $\boldsymbol{q_{>}}$ is the maximum value of q (ultraviolet cut-off), and a mixed membrane of AB separates into two equal-sized regions of disordered A and ordered B with $\boldsymbol{\kappa_{AB} \approx \kappa_A < \kappa_B}$. Undulating membranes favor a mixed state, indicating that undulation-suppressed membranes tend to shift to a separated state. It is known that a thermally undulating membrane can be described by a set of independent harmonic oscillators with a spring constant of $\boldsymbol{\kappa q^4}$ (Safran, 2002). Gordon et al., then developed the free energy using a harmonic potential $\boldsymbol{mh^2/2}$ as the confinement of undulation, where ***h(x,y)*** is the local deviation and $\boldsymbol{m}$ shows the strength of the confinement (Gordon et al., 2008). Thus, a spring constant of the undulation-suppressed membrane is $\boldsymbol{\kappa q^4 + m}$. The confinement-dependent undulation term is obtained by

$$\boldsymbol{f}_{\mathbf{und}} \cong \frac{\pi k_{\mathrm{B}} T}{4a^2} \left\{ \ln \frac{\alpha + \tilde{m}}{1 + \tilde{m}} + 2\sqrt{\tilde{m}/\alpha} \arctan \frac{1}{\sqrt{\tilde{m}/\alpha}} - 2\sqrt{\tilde{m}} \arctan \frac{1}{\sqrt{\tilde{m}}} \right\}, \qquad (7)$$

where the stiffness factor $\alpha = \kappa_B/\kappa_A$ and the dimensionless confinement parameter $\tilde{m} = m/\kappa q_>^4$.

Figure 4-2 shows the confinement dependence of the free energy with S_o (α=10) (Dimova et al., 2000) and L_o (α=2) domains (Roux et al., 2005). f_{und} is positive and decreases when the undulation is suppressed by osmotic pressure ($\tilde{m}$ increases). Without osmotic pressure, even if f_{mix} is negative to induce phase separation, the total free energy Δf may become positive to show the homogeneous phase. After the application of osmotic pressure, f_{und} decreases and Δf becomes negative to produce phase separation. The undulation contribution depends on the rigidity of the ordered domains. The S_o phase with high rigidity has higher f_{und} than the L_o phase (Fig. 4-2). Thus, osmotic pressure changes the total free energy of L_o/L_d phase separation to be negative more easily than that of S_o/L_d phase separation, indicating that L_o/L_d phase separation shows a greater response to osmotic pressure, which agrees with our experimental results (Fig. 3-2). Soon, it will be necessary to interpret this phenomenon by a theoretical model, taking into account undulation suppression and lipid phase transition.

Moreover, there were several reports on the effects of other stimuli on phase behavior and line tension. Honerkamp-Smith et al. showed that line tension decreased to zero when the temperature approached the miscibility temperature (Honerkamp-Smith et al., 2008). Line tension is also reported to be affected by chemical stimuli, resulting in a

shift of the miscibility temperature (Goh et al., 2013; Hamada et al., 2011; Ostroumova et al., 2014). Previous studies proposed that an increase in the palmitic acid composition can increase line tension by substitution of cholesterol in the L_o phase, whereas the addition of oleic acid and phytanic acid can significantly decrease line tension by disturbing L_o phase (Shimokawa et al., 2017). Similarly, it was also suggested that hybrid lipids or phospholipids with saturated and unsaturated acyl chains can reduce the line tension by reducing the order of the L_o phase (Hassan-Zadeh et al., 2014; Usery et al., 2017). The line tension can also be reduced by vitamin E (tocopherol) and local anesthetics, including lidocaine and tetracaine which decrease the interfacial free energy (Sugahara et al., 2017; Yang et al., 2016). Different lipid compositions resulted in different properties of lipid domains and patterns of phase separation (Goh et al., 2013; Konyakhina et al., 2011). The conformational change in a photo-responsive membrane lipid was reported to change the line tension and control the emergence/disappearance of domains (Hamada et al., 2011). Notably, here we controlled the line tension by osmotic pressure without chemical modification. This may lead to an understanding of the regulation of line tension under isothermal conditions, such as in cell membranes. Additionally, it was suggested that phase separation can be affected by some physical stimuli including, hydrostatic force, membrane adherence, and tension modification. It was believed that an increase in hydrostatic pressure was reported to induce phase separation via the increase of L_o and L_d height mismatch (McCarthy et al., 2015). Gordon et al. reported that, among various

lipid compositions, domain formation can be enhanced when two membranes adhere (Gordon et al., 2008). The adhesion of membranes on a surface was suggested to increase membrane tension, suppress undulation, and produce lipid heterogeneity (Gordon et al., 2015). Notably, a study on tension modification using micropipette puller showed the contradict results that an increase of membrane tension can reduce the miscibility temperature (Portet et al., 2012). The opposite behaviors of tensed membranes were suggested that the micropipette technique induces strong tension that increases the surface area of lipids over the suppression of membrane undulation (Gordon et al., 2015).

Notably, we observed that, at 40% Chol, the miscibility temperature under tension was higher than the melting temperature of DPPC. This may be attributed to a tension-induced change in the tie line of the phase diagram. The tie line determines the Chol concentration of the separated L_o phase (Veatch et al., 2006).

This is the first report to examine the effects of osmotic swelling on the line tension of membrane domains. The enhance of phase separation by osmotic swelling are complementary to other physical stimuli including membrane adhesion and hydrostatic force. This type of physical stimulus can easily occur in the living cell, in particular, the hemostasis mechanism. Results are beneficial for understanding insight in lipid membrane properties itself in the regulation of the mechanism.

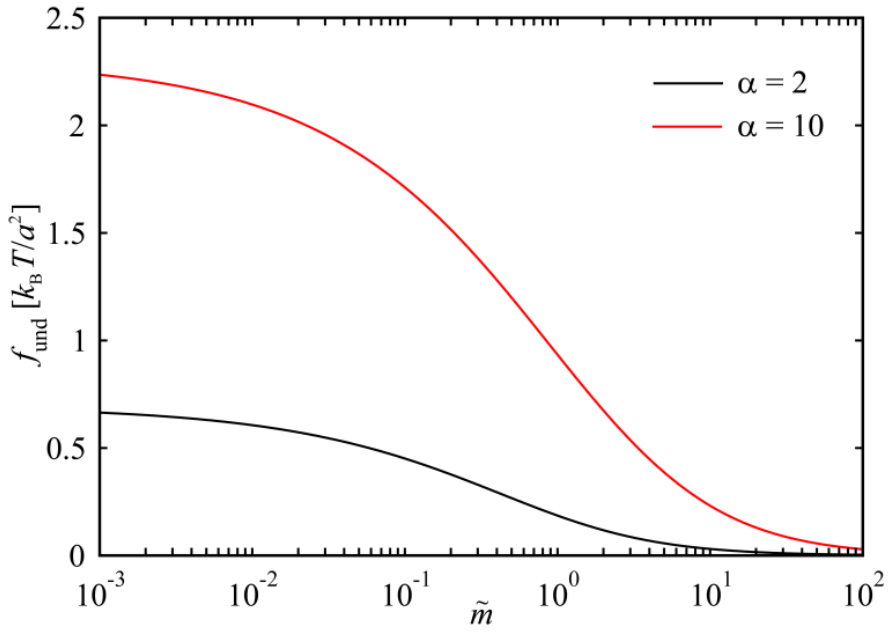

Figure 4-2 Confinement dependence of the undulation term of the free energy for membranes with S_o (α=10) and L_o (α =2) domains. $\tilde{m}$ is the dimensionless confinement parameter.

Reference

Dimova, R., Pouligny, B., & Dietrich, C. (2000). Pretransitional effects in dimyristoylphosphatidylcholine vesicle membranes: Optical dynamometry study. *Biophysical Journal*, *79*(1), 340–356. https://doi.org/10.1016/S0006-3495(00)76296-5

Esposito, C., Tian, A., Melamed, S., Johnson, C., Tee, S. Y., & Baumgart, T. (2007). Flicker spectroscopy of thermal lipid bilayer domain boundary fluctuations. *Biophysical Journal*, *93*(9), 3169–3181. https://doi.org/10.1529/biophysj.107.111922

García-Sáez, A. J., Chiantia, S., & Schwille, P. (2007). Effect of line tension on the lateral organization of lipid membranes. *Journal of Biological Chemistry*, *282*(46), 33537–33544. https://doi.org/10.1074/jbc.M706162200

Goh, S. L., Amazon, J. J., & Feigenson, G. W. (2013). Toward a better raft model: Modulated phases in the four-component bilayer, DSPC/DOPC/POPC/CHOL. *Biophysical Journal*, *104*(4), 853–862. https://doi.org/10.1016/j.bpj.2013.01.003

Gordon, V. D., Deserno, M., Andrew, C. M. J., Egelhaaf, S. U., & Poon, W. C. K. (2008). Adhesion promotes phase separation in mixed-lipid membranes. *Epl*, *84*(4). https://doi.org/10.1209/0295-5075/84/48003

Gordon, V. D., O'Halloran, T. J., & Shindell, O. (2015). Membrane adhesion and the formation of heterogeneities: Biology, biophysics, and biotechnology. *Physical Chemistry Chemical Physics*, *17*(24), 15522–15533. https://doi.org/10.1039/c4cp05876c

Hamada, T., Sugimoto, R., Nagasaki, T., & Takagi, M. (2011). Photochemical control of membrane raft organization. *Soft Matter*, *7*(1), 220–224. https://doi.org/10.1039/c0sm00797h

Hassan-Zadeh, E., Baykal-Caglar, E., Alwarawrah, M., & Huang, J. (2014). Complex roles of hybrid lipids in the composition, order, and size of lipid membrane domains. *Langmuir*, *30*(5), 1361–1369. https://doi.org/10.1021/la4044733

Hed, G., & Safran, S. A. (2003). Initiation and dynamics of hemifusion in lipid bilayers. *Biophysical Journal*, *85*(1), 381–389. https://doi.org/10.1016/S0006-3495(03)74482-8

Honerkamp-Smith, A. R., Cicuta, P., Collins, M. D., Veatch, S. L., Den Nijs, M., Schick, M., & Keller, S. L. (2008). Line tensions, correlation lengths, and critical exponents in lipid membranes near critical points. *Biophysical Journal*, *95*(1), 236–246. https://doi.org/10.1529/biophysj.107.128421

Konyakhina, T. M., Goh, S. L., Amazon, J., Heberle, F. A., Wu, J., & Feigenson, G. W. (2011). Control of a nanoscopic-to-macroscopic transition: Modulated phases

in four-component DSPC/DOPC/POPC/Chol giant unilamellar vesicles. *Biophysical Journal*, *101*(2), L8. https://doi.org/10.1016/j.bpj.2011.06.019

Kuzmin, P. I., Akimov, S. A., Chizmadzhev, Y. A., Zimmerberg, J., & Cohen, F. S. (2005). Line tension and interaction energies of membrane rafts calculated from lipid splay and tilt. *Biophysical Journal*, *88*(2), 1120–1133. https://doi.org/10.1529/biophysj.104.048223

Lee, D. W., Min, Y., Dhar, P., Ramachandran, A., Israelachvili, J. N., & Zasadzinski, J. A. (2011). Relating domain size distribution to line tension and molecular dipole density in model cytoplasmic myelin lipid monolayers. *Proceedings of the National Academy of Sciences of the United States of America*, *108*(23), 9425–9430. https://doi.org/10.1073/pnas.1106368108

McCarthy, N. L. C., Ces, O., Law, R. V., Seddon, J. M., & Brooks, N. J. (2015). Separation of liquid domains in model membranes induced with high hydrostatic pressure. *Chemical Communications*, *51*(41), 8675–8678. https://doi.org/10.1039/c5cc02134k

McMullen, T. P. W., & McElhaney, R. N. (1995). New aspects of the interaction of cholesterol with dipalmitoylphosphatidylcholine bilayers as revealed by high-sensitivity differential scanning calorimetry. *BBA - Biomembranes*, *1234*(1), 90–98. https://doi.org/10.1016/0005-2736(94)00266-R

Ostroumova, O. S., Chulkov, E. G., Stepanenko, O. V., & Schagina, L. V. (2014). Effect of flavonoids on the phase separation in giant unilamellar vesicles formed from binary lipid mixtures. *Chemistry and Physics of Lipids*, *178*, 77–83. https://doi.org/10.1016/j.chemphyslip.2013.12.005

Portet, T., Gordon, S. E., & Keller, S. L. (2012). Increasing membrane tension decreases miscibility temperatures; An experimental demonstration via micropipette aspiration. *Biophysical Journal*, *103*(8), L35–L37. https://doi.org/10.1016/j.bpj.2012.08.061

Roux, A., Cuvelier, D., Nassoy, P., Prost, J., Bassereau, P., & Goud, B. (2005). Role of curvature and phase transition in lipid sorting and fission of membrane tubules. *EMBO Journal*, *24*(8), 1537–1545. https://doi.org/10.1038/sj.emboj.7600631

Safran, S. A. (2002). Statistical thermodynamics of soft surfaces. *Surface Science*, *500*(1–3), 127–146. https://doi.org/10.1016/S0039-6028(01)01535-7

Shimokawa, N., Mukai, R., Nagata, M., & Takagi, M. (2017). Formation of modulated phases and domain rigidification in fatty acid-containing lipid membranes. *Physical Chemistry Chemical Physics*, *19*(20), 13252–13263. https://doi.org/10.1039/c7cp01201b

Stottrup, B. L., Tigrelazo, J., Bagonza, V. B., Kunz, J. C., & Zasadzinski, J. A.

(2019). Comparison of Line Tension Measurement Methods for Lipid Monolayers at Liquid-Liquid Coexistence. *Langmuir*, *35*(48), 16053–16061. https://doi.org/10.1021/acs.langmuir.9b01696

Sugahara, K., Shimokawa, N., & Takagi, M. (2017). Thermal stability of phase-separated domains in multicomponent lipid membranes with local anesthetics. *Membranes*, *7*(3). https://doi.org/10.3390/membranes7030033

Tsai, W. C., & Feigenson, G. W. (2019). Lowering line tension with high cholesterol content induces a transition from macroscopic to nanoscopic phase domains in model biomembranes. *Biochimica et Biophysica Acta - Biomembranes*, *1861*(2), 478–485. https://doi.org/10.1016/j.bbamem.2018.11.010

Usery, R. D., Enoki, T. A., Wickramasinghe, S. P., Weiner, M. D., Tsai, W. C., Kim, M. B., Wang, S., Torng, T. L., Ackerman, D. G., Heberle, F. A., Katsaras, J., & Feigenson, G. W. (2017). Line Tension Controls Liquid-Disordered + Liquid-Ordered Domain Size Transition in Lipid Bilayers. *Biophysical Journal*, *112*(7), 1431–1443. https://doi.org/10.1016/j.bpj.2017.02.033

Veatch, S. L., Gawrisch, K., & Keller, S. L. (2006). Closed-loop miscibility gap and quantitative tie-lines in ternary membranes containing diphytanoyl PC. *Biophysical Journal*, *90*(12), 4428–4436. https://doi.org/10.1529/biophysj.105.080283

Yang, S. T., Kiessling, V., & Tamm, L. K. (2016). Line tension at lipid phase boundaries as driving force for HIV fusion peptide-mediated fusion. *Nature Communications*, *7*. https://doi.org/10.1038/ncomms11401

Chapter 5 Modification of line tension in mixed lipid membranes

Chapter 5 Modification of line tension in mixed lipid membranes

Introduction

A fatty acid is an essential component of cellular membranes to determine the physical properties of cellular membranes. Because of differences in the lipid complexity membrane, some bacteria are alive and grow at high temperatures, whereas some of them are viable at low temperatures. Cellular membrane made of lipids from the combination of both de novo synthesis of phospholipids and their remodeling be diacylation/reacylation cycles (Hulbert et al., 2014). It was suggested that dietary polyunsaturated fatty acids incorporate into the cell membrane of the human cell membrane (Cao et al., 2006). Relationships of the diets and the properties of the membranes are little investigated. It is well-known that unsaturated fatty acid is beneficial to prevent chronic diseases such as diabetes and cardiovascular disease but the molecular mechanism behind remains unknown. The incorporated into the cell membrane of unsaturated fatty acid and manipulated membrane functions is suggested to be a possible mechanism (Jump, 2002). Effects of polyunsaturated fatty acid as the unsaturated acyl chain to phase separation have been investigated (Wassall & Stillwell, 2009; Georgieva et al., 2015; Levental et al., 2016). Besides, that treated membranes with saturated fatty acids can cause the membranes tighter packing whereas treated those with unsaturated fatty acids, the packing is reduced (Onuki et al., 2008). Since the kink structure of unsaturated fatty

acid can partition into the membranes by reducing the van der Waals interaction between the hydrophobic chains, the membrane fluidity is increased. Polyunsaturated fatty acids produce stronger effects on the membrane fluidity than monounsaturated fatty acids. Consequently, the affinity of cholesterol and polyunsaturated fatty acids is much lower than those of monounsaturated fatty acids (Wassall et al., 2004). It was suggested that both *cis* and *trans* conformation interfere mainly in the hydrophobic region. Indeed, *cis* isomer of unsaturated fatty acid can be synthesized in eukaryote whereas *trans* isomer of unsaturated fatty acid can be obtained from an exogenous source such as in meat, dairy products, and margarine. Intake *trans* fats are believed to cause negative effects on health by altered the plasma lipoprotein profile. Also, *trans* fats have received a lot of attention due to their alteration of the hydrophobic region on lipid membranes. Due to their geometry structure, acyl chains of *trans* conformation can more possibly extend whereas those of *cis* isomer is likely to kink. Therefore, based on the area/molecule *cis* conformation is larger than *trans* conformation. Both fatty acid as the unsaturated acyl chain localized in L_d unsaturated lipid rich phase. The acyl pack order of *trans* conformation tends to more ordered and has more van der Waals interaction than *cis* (Soni et al., 2009). While *cis* conformation tends to more fluidity than *trans* (Smith et al., 2014). Subsequently, the membrane containing *cis* and *trans* conformation provide different physical properties. Modification of the lipid composition of the membranes disturbs the protein activity by changing the hydrophobic region (Killian, 1998), domain formation (Zaloga et al., 2006), membrane fluidity, and acyl chain packing (Roach et al., 2004).

The partitioning of various types of fatty acid including hybrids lipid (lipid with one saturated acyl chain and one unsaturated acyl chain) (Shimokawa et al., 2015), saturated fatty acids, branch chain, cis-isomer, and trans-isomer addition in membrane model has been examined (Shimokawa et al., 2017). Their transition temperature and line tension have also been compared. Hybrid lipids had been expected to localize between L_o and $L_{d,}$ but it was found that increase palmitoyloleoyl-phosphatidylcholine (POPC) can lower the GP value of the L_o phase. This can imply that POPC molecules partitioned in the L_o phase and disturbing the chain ordering of the L_o phase. The addition of palmitic acid (saturated fatty acid) and elaidic acid (trans-isomer of unsaturated fatty acid) exclude cholesterol from the L_o phase. Palmitic acid provides stronger effects than elaidic acid due to the attraction between DPPC and palmitic acid is stronger than those of elaidic acid. The miscibility temperature and line tension show higher than without addition. In contrast, small amounts of oleic acid (*cis* isomer of unsaturated fatty acid) and phytanic acid (branched fatty acid) partitioned into the L_o phase and disrupt the order chain. Therefore, the difference in membrane physical properties between L_o and L_d phase is smaller. Their miscibility temperature and line tension are lower.

In this study, we focused on the monounsaturated fatty acid and their reduced line tension. It is very interesting in determining the effects of various chain length and cis position of monosaturated fatty acid and also their effects under osmotic tension swelling condition to the partition of them in a model membrane.

Materials and Methods

Materials

1,2-Dioleoyl-*sn*-glycero-3-phosphocholine (DOPC), 1,2-dipalmitoyl-*sn*-glycero-3-phosphocholine (DPPC), and cholesterol (Chol) were purchased from Avanti Polar Lipids (Alabaster, AL). Rhodamine (Rho)-1,2-dihexadecanoyl-*sn*-glycero-3-phosphoethanolamine (DHPE) (rhodamine-DHPE, triethylammonium) and 1,2-dipalmitoyl-*sn*-glycero-3-phosphoethanolamine-*N*-(7-nitrobenz-2-1,3-benzoxadiazol-4-yl) (ammonium salt) (NBD-PE) was obtained from Thermo Fisher Scientific (Waltham, US) and Avanti Polar Lipids, respectively. D(+)-Glucose, oleic acid (C18:1, cis 9) (OA), petroselinic acid (C18:1, cis 6) (PeA), cis-vaccenic acid (C18:1, cis 11) (VA), and palmitoleic acid (C16:1, cis 9) (PA) were purchased from Nacalai Tesque (Kyoto, Japan). The eicosenoic acid (C20:1, cis 9) (EA) was purchased from Larodan Fine Chemicals (Malmö, Sweden). Figure 5-1 showed the chemical structures used in this study. Milli-Q water (Specific resistance ≥18 MΩ) used in this study was from a Millipore Mill-Q purification system.

Vesicles preparation and osmotic tension application

Vesicles were prepared using the natural swelling method. 0.2 mM lipids and 1 μM fluorescence probe (rhodamine-DHPE and NBD-PE) were dissolved in chloroform. The organic solvent was evaporated using a flow of nitrogen gas and the formed lipid films are further dried under vacuum for 3 h. The films were then pre-heated using 5 μL of Milli-Q water for 10 minutes at 55°C and hydrated using 200 mM of

Glucose solution for 3 h at 37°C. The tense vesicles were produced by mixed the vesicle solution with the Milli-Q water at the ratio 1:9 for ΔC= 180.

Microscope Observation

The vesicle solution without osmotic tension and the hypotonic vesicle solution with osmotic tension were comparisons observed under the microscope. They were placed on a glass slide and covered by another coverslip with silicone spacing of ca. 0.1 mm. Their phase behaviors were examined using a fluorescent microscope (IX71, Olympus, Japan) for further line tension analysis and a confocal laser scanning microscope (FV-1000, Olympus, Japan) at room temperature (~23 ± 2 ℃). In this study, rhodamine-DHPE and NBD-PE were used as fluorescent dyes. A standard filter set, UMWIG, with excitation wavelength λ_{ex}=530-550 nm and emission wavelength λ_{em} =575 nm was used to monitor the fluorescence of Rhodamine-DHPE, and another filter, U-MNIBA, with λ_{ex} =470-495 nm and λ_{em} =510-550 nm, was used for the NBD-PE dye. The resolution is at 1 pixel 0.16 μm for 60X objective lens. The effects of length and cis position of hydrophobic chain on membrane model were studied and compared.

Flicker spectroscopy of domain boundary fluctuation

Line tension at the domain boundary fluctuation was obtained and analyzed from a movie of >3 sec (>90 frames, 30 frames/sec) of a phase-separated domain. The resolution is at 1 pixel = 0.1 μm (100X, objective lens). The radius of the domain

was traced along the perimeters of binary images using ImageJ software. Line tension results at domain boundary fluctuation were then calculated using developed in-house software by plotted the domain radius (r) as the function of the polar angle (ψ) (Stottrup et al., 2007). The fluctuating domain boundary was presented in terms of a Fourier series expansion:

$$r(\psi) = r_{\mathrm{av}}\left[1 + a_o + \sum_{k=1}^{\infty} a_k \cos(k\psi) + \sum_{k=1}^{\infty} b_k \sin(k\psi)\right] \qquad (2)$$

where $\boldsymbol{r_{av}}$ is the average domain radius, $\boldsymbol{k}$ is the mode number, and $\boldsymbol{a_k}$ and $\boldsymbol{b_k}$ are Fourier coefficients. The fluctuation and the excess free energy are expressed as

$$\Delta F \simeq \frac{\pi r_{\mathrm{av}}}{2}\gamma \sum_{k=2}^{\infty} (k^2 - 1)\,(a_k^2 - b_k^2) \qquad (3)$$

where $\boldsymbol{\gamma}$ is the line tension. The free energy for each independent mode is $\boldsymbol{k_B T}$ from the generalized equipartition theorem. Therefore, we obtain:

$$\langle a_k^2 \rangle + \langle b_k^2 \rangle = \frac{2k_{\mathrm{B}}T}{\pi r_{\mathrm{av}}\gamma}\left(\frac{1}{k^2 - 1}\right) \qquad (4)$$

where $\langle \ldots \rangle$ is the average value of all images. The line tension $\boldsymbol{\gamma}$ can be obtained by applying linear regression to the relationship of the mode number $\boldsymbol{k}$ and the Fourier coefficients $\boldsymbol{a_k}$ and $\boldsymbol{b_k}$, as described by equation (4).

DSC Measurements

300 mM of DPPC, Chol, and each type of fatty acid (FA) were dissolved in chloroform. These compositions were mixed at the desired lipid ratio at the total volume of 30 μL. The solvents are evaporated under the Nitrogen gas fuming, and the films were completely dried under the vacuum for at least 3 hr. Then, the films were hydrated using the 200 mM glucose for 60 μL which make the final concentration of lipids were at 150 mM. All lipid solutions were homogenized using vortex and sonicated at 60°C for 1 hr before analysis using DSC. The ratios examined were DPPC/Chol/FA 90/10/0, 85/10/5, 80/10/10. And 75/10/15.

The thermographs were obtained by a DSC822 (Mettler Toledo, Switzerland) from 20°C to 60°C (3 cycles). The heating and cooling rates were at 5 °Cmin^{-1}. 12-15 μL of lipid solutions were weight onto the aluminum pans whereas the equivalent weight of 200 mM glucose solutions was used as the reference cell. Samples were run in triplicate and results were normalized by the weight of each sample.

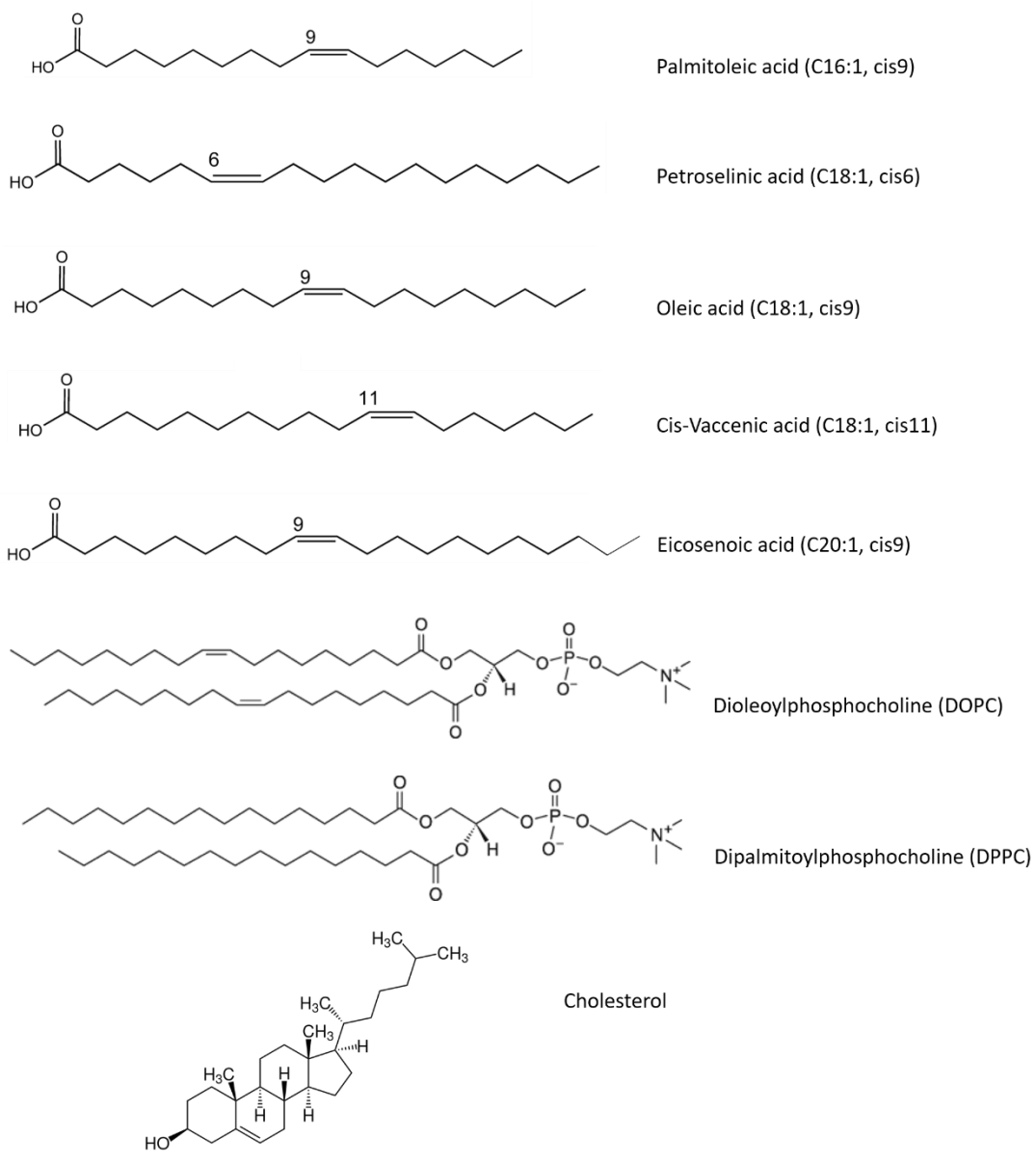

Figure 5-1 Chemical structures of fatty acids

Results

Effect of chain length to the partition of fatty acids in phase separation

A series of fatty acid (FAs): palmitoleic acid (PaA, C16:1, cis 9), oleic acid (OA, C18:1, cis 9), and eicosenoic acid (EA, C20:1, cis 9) were used to determine the effects of carbon chain length on DOPC/DPPC/Chol phase separation, because the positions of double bond in the hydrocarbon chains are the same and the lengths between the double bond and the end of the hydrocarbon tail are different. Since the tail structure of the DOPC structure is oleic acid, DOPC is replaced by OA (C18:1, cis 9) at 10%, 20%, and 30% in DOPC/DPPC/Chol 40/40/20 (Figure 5-2 (a) and 5-3 (a)). Other FAs were also replaced in DOPC to compare. The observation results are in agreement with previous work that replaced oleic acid between 10% to 30% with DOPC can produce the phase separation whereas no phase separation structure has been seen at 40% OA (C18:1, cis 9) substitution. The domain fluctuation increases as the increased content of fatty acids. This domain fluctuation results are consistent with the previous results. To observe both L_o phase and L_d phase, we used confocal microscopy (Figure 5-2(b) and 5-3(b)). In normal conditions without osmotic pressure, addition 10% of OA (C18:1, cis 9), PaA (C16:1, cis 9), and EA (C20:1, cis 9) showed the more flatted shape of the L_o phase (green color) and curved shape of the L_d phase (red color). The line tension is slightly decreased so the vesicles are deformed from the spherical shape. Although the domain boundary length is increased for deformed vesicles, the rigid L_o phase can be flat shape and the decrease of the curvature energy overcomes the increase

of the line energy. When increasing fatty acid content, the line tension can adequately suppress leading to the number of domains is increased. Therefore, the vesicles more approach spherical. Figure 5-2 showed that OA (C18:1, cis 9) and PaA (C16:1, cis 9) containing vesicles provide similar phase separation behaviors. It can be implied that they mainly partition in the L_d phase and a small amount of them can also partition in the L_o phase and destabilize it. The small amount of them disturbed the ordered phase and enhanced the domain boundary fluctuation. On the contrary, increase the content of such the long chain as EA (C20:1, cis 9) disrupts the stability of vesicle production as shown in the smaller number of vesicles and the smaller size of vesicles. Also, some large aggregation sediments in the test tube. Moreover, the increase of EA can enhance the production of the S_o/L_d phase. This can imply the EA (C20:1, cis 9) might have strong interaction to exclude cholesterol from DPPC-rich phase. This behavior is essentially the same as elaidic acid as reported previously. Also, elaidic acid has a double bond in its hydrocarbon tail, but trans isomer. Figure 5-2(e) showed the microscopy images obtained by the confocal microscope of three coexisting phases: a dark region (EA-DPPC rich phase), a green region (Chol-DPPC rich phase), and a red region (DOPC rich phase). The responsiveness of osmotic stress microscopic images has been shown that tension inside vesicles can overcome the flatted shape of the L_o phase in all percentage of addition. (Figure 5-2(c)). To understand the partition of fatty acids in L_o/L_d phase more precisely, the line tension analysis was performed.

Effect of chain length to the partition of fatty acids in line tension

Line tension at the domain boundary could give some important insights into the partition of lipids at a molecular level. Therefore, the effects of the chain length will be further compared and explain by line tension analysis. The line tension analysis in this study is measured based on the flicker spectroscopy of domain boundary fluctuation. Only the circular domains were included in this study. Ten of them for each condition were recorded for more than 2 sec (30 frames/sec) at room temperature. Their radius was traced and analyzed using ImageJ software, and line tension values were calculated using eq 2-4. The line tension values are summarized in figure 5-2(d). We measured line tension around ten vesicles randomly. Without fatty acid addition, the average line tension (γ) of DOPC/DPPC/Chol 40/40/20 was around 5.58 ± 1.72 pN and 8.91 ± 2.64 pN without and with osmotic pressure, respectively.

In OA (C18:1, cis 9) system, the obtained averaged values are $\gamma = 3.80 \pm 1.91$ pN (OA= 10%), $\gamma = 2.34 \pm 1.91$ pN (OA= 20%), and $\gamma = 4.46 \pm 2.05$ pN (OA= 30%). Addition of OA (C18:1, cis 9) reduces line tension. 20% OA addition could be the saturated amount to partition in the L_o phase. Therefore, the increase in OA to 30% does not affect much to line tension value. In response to the osmotic pressure of the OA system, the obtained values are $\gamma = 6.30 \pm 3.26$ pN (OA= 10%), $\gamma = 2.87 \pm 2.34$ pN (OA= 20%), and $\gamma = 4.49 \pm 2.70$ pN (OA= 30%). Osmotic pressure can enhance the line tension values to increase especially at 10% of OA additional in lipid membrane. The response showed lower in the addition of 20% and 30% OA

containing vesicles. The tendency of line tension upon osmotic pressure are not quite clear by line tension experiments.

Whereas in shorter chain of PaA (C16:1, cis 9), we obtained $\gamma = 2.65 \pm 1.04$ pN (PaA= 10%), $\gamma = 3.22 \pm 0.82$ pN (PaA= 20%), and $\gamma = 5.76 \pm 3.14$ pN (PaA= 30%). It was shown that the addition of PaA can reduce line tension, but the reduction seems to less than OA. 10% addition of PaA showed the highest disturbance of L_o phase whereas an increased amount of PaA does not more decrease line tension. This might be because PaA is more difficult to locate in the L_o phase. We found that osmotic pressure can also enhance the line tension in the PaA system especially at 10% addition of PaA. The enhance of line tension can be negligible in the higher content of PaA like the OA system. The values are $\gamma = 4.56 \pm 2.39$ pN (PaA= 10%), $\gamma = 3.78 \pm 2.07$ pN (PaA= 20%), and $\gamma = 6.05 \pm 2.88$ pN (PaA= 30%).

Since our line tension analysis values are slightly higher than the previous work. We found that some domains fluctuate, and some domains do not. Both conditions of domains were calculated together lead to a high value of line tension. Therefore, we then estimated the fraction of the fluctuation domain for each ratio of each fatty acids (Table. Since the minimum line tension value of DOPC/DPPC/Chol was 2.85 pN. Therefore, we will define the line tension value of less than 2.85 pN as the fluctuating domain. The fraction of fluctuation domain of OA and PaA are showed in Table 5-1.

It is difficult to obtain the circular domains with suitable size in EA systems. Also,

most of them are S_o/L_d phase so the line tension cannot be calculated in EA system. These line tension results are further discussed in the discussion part. The effects of the different chain length of fatty acids to the incorporated in the ordered phase also investigated using DSC.

Effect of chain length of fatty acids to the thermostability of lipid membranes

DSC was also used to determine the effects of FAs on the lipid membranes. Figure 5-4 clearly showed the fitting asymmetric thermograph of DPPC/Chol 90/10 (blue color) which consists of two Gaussian functions. The sharp gray peak was assigned as the S_o phase (41°C) whereas the red board peak was indicated as the L_o phase locating at around 42°C. This result consistent with a previous study (McMullen, T. P. W. et al., 1995).

For OA (C18:1, cis 9), the thermographs and the results of peak deconvolution were shown in Figure 5-5 b. Although we assume that the thermograph obtained experimentally is consisting of two peaks, the second peaks denoted by red line is much weaker than the intensity of the first peak denoted by black lines. Therefore, we consider that there is only one peak, and this means that all components, DPPC, Chol, and OA, are well-mixed each other. Also, an increase in OA concentration leads to a decrease in the transition temperature. Although many OA is easily partitioning in the L_d phase, DSC results showed that some OA molecules can partition in the L_o phase and destabilize the L_o phase (Figure 5-7).

For PaA (C16:1, cis 9), results are complementary to the OA system. PaA can also

incorporate with DPPC and cholesterol (Figure 5-5 a). The Gaussian function of the narrow and board peaks are in parallel with OA results. The main difference is that PaA strongly reduces in the transition temperature (Figure 5-7). This result contradicts the line tension results. Since PaA more decreases the transition temperature than OA, PaA destabilizes L_o phase than OA. Therefore, we speculate that most of PaA is distributed to the L_d phase and the amount of PaA included in the L_o phase may be smaller than that of OA when DOPC is present.

EA (C20:1, cis 9) showed contradict results from OA and PaA. The fitting result showed two clear peaks. Increase concentration of EA, the second peak (at a higher temperature) become stronger than the first peak (at a lower temperature) (Figure 5-5 c). We assigned the second peak as the EA-rich phase which can exclude cholesterol as the presence of the S_o/L_d phase. This character is similar to saturated fatty acid (Shimokawa et al., 2017). EA did not stabilize the L_o phase like OA and PaA, and its transition temperature did not decrease significantly (Figure 5-7).

Effect of cis position to the partition of fatty acids in phase separation

Next, the effects of three fatty acids (FA) with different cis positions: petroselinic acid (PeA, C18:1, cis 6), oleic acid (OA, C18:1, cis 9), and cis-vaccenic acid (VA, C18:1, cis 11), on DOPC/DPPC/Chol phase separation were determined. They were replaced with DOPC at 10, 20, and 30%, similarly (Figure 5-3(a)). Their fractions of domain fluctuation are showed on Table 5-1.

The elevated content of VA (C18:1, cis 11) enhances the domain fluctuation which is compatible with the results of OA and PaA. Addition less amount of VA showed

the deformation shape with the flatted part of the L_o phase (green color) and the curved part of the L_d phase (red color) (Figure 5-3(b)). Whereas the vesicles become more spherical shape when increase contents of VA due to those increasing content reduce sufficient line tension and producing many domains. None of S_o/L_d phase separation has been found in vesicles containing VA.

In contradiction, PeA (C18:1, cis 6) containing vesicles does not show the increase of fluctuation as in OA, PA, and VA cases. The fluctuation in this system is not significant. Also, none of the S_o/L_d phase separation has been obtained. The confocal laser scanning microscope images showed the vesicles become deformed shape with a small content of PeA. Increase the content of PeA, the vesicles tend to become a spherical shape. But the turning to spherical shape by this fatty acid might from different reasons of OA, PA, and VA. The response of these various cis position fatty acids upon osmotic pressure clearly showed in figure 5-3(c). Their line tension might be increased from turning to the spherical shape of vesicles. We further performed line tension analysis for more precisely understand about their partition in the biomembranes vesicles.

Effect of cis position to the partition of fatty acids in line tension

The line tension of membrane containing fatty acid with the different cis position was analyzed by the same procedure as in the case of OA and PaA. Ten circular shape domains from different vesicles were includes. Figure 5-3(d) exhibits the line tension comparing among different cis positions.

As a result, the line tension values are $\gamma = 4.11 \pm 2.65$ pN (VA= 10%), $\gamma = 3.10 \pm 1.72$ pN (VA= 20%), and $\gamma = 3.18 \pm 2.66$ pN (VA= 30%). It was shown that the addition of VA (C18:1, cis 11) can reduce line tension, especially in 10% and 20%. However, the reduction is less than OA and PaA. Osmotic pressure can enhance the line tension values in membrane containing VA. The obtained values are $\gamma = 4.22 \pm 3.13$ pN (VA= 10%), $\gamma = 5.88 \pm 3.79$ pN (VA= 20%), and $\gamma = 5.78 \pm 3.85$ pN (VA= 30%). Results showed that line tension is enhanced as the increase in VA concentration under osmotic pressure. This might be because VA incorporates in L_o phase less than OA and PaA so 20% additional of VA is not the saturated ration. On the contrary, VA is strongly destabilizing the L_o phase than OA and PaA. As increase VA concentration, a higher amount of VA includes in the L_o phase. The line tension seems to more decrease without osmotic pressure and more increases with osmotic pressure as a higher content of VA.

For PeA (C18:1, cis 6) systems, the line tension without osmotic pressure values are $\gamma = 3.81 \pm 1.48$ pN (PeA= 10%), $\gamma = 5.60 \pm 1.75$ pN (PeA= 20%), and $\gamma = 5.47 \pm 2.28$ pN (PeA= 30%). Line tension is suppressed only at the addition of 10% PeA. In contrast, increase PeA content to 20% and 30%, line tension values are comparable to control (DOPC/DPPC/Chol). In the response to the osmotic pressure of membrane containing PeA, the obtained results are $\gamma = 3.90 \pm 2.71$ pN (PeA= 10%), $\gamma = 4.24 \pm 1.83$ pN (PeA= 20%), and $\gamma = 2.72 \pm 1.66$ pN (PeA= 30%). Interestingly, tension enhances the line tension value inversely as the increase of PeA content. To understand more precisely, we examine effects of cis position of fatty acid on the transition temperature using DSC in the next part.

Effect of cis position of fatty acids to the thermostability of lipid membranes

In this part, we would like to understand effects of FAs on the thermostability of lipid membranes using DSC measurements. As mention above, we assumed that the obtained thermograph is composed of two Gaussian functions (Figure 5-4).

The results of the increase in the cis position of VA (C18:1, cis 11) showed obvious two noticeable peaks (Figure 5-6 b). As the increase of VA concentration, the second peak (at a higher temperature) become clearer. We assigned the second peak as the VA-rich phase. From DSC results, it can be implied that VA localized in the L_o phase less than OA. Even a small amount of VA includes in the L_o phase, the line tension value showed that VA is strongly disturbed in the L_o phase.

The fitting results of the thermographs of DPPC/Chol/PeA (C18:1, cis 6) present as one peak as the OA cumulative peak (Figure 5-6 a). But the two Gaussian thermographs of PeA are distinct from OA and VA. Both L_o and S_o peaks are similarly dominant. Therefore, PeA can incorporate with the DPPC and cholesterol. However, PeA does not destabilize the L_o phase as OA as shown in the transition temperature which is not decreased as the increase of PeA concentration (Figure 5-7).

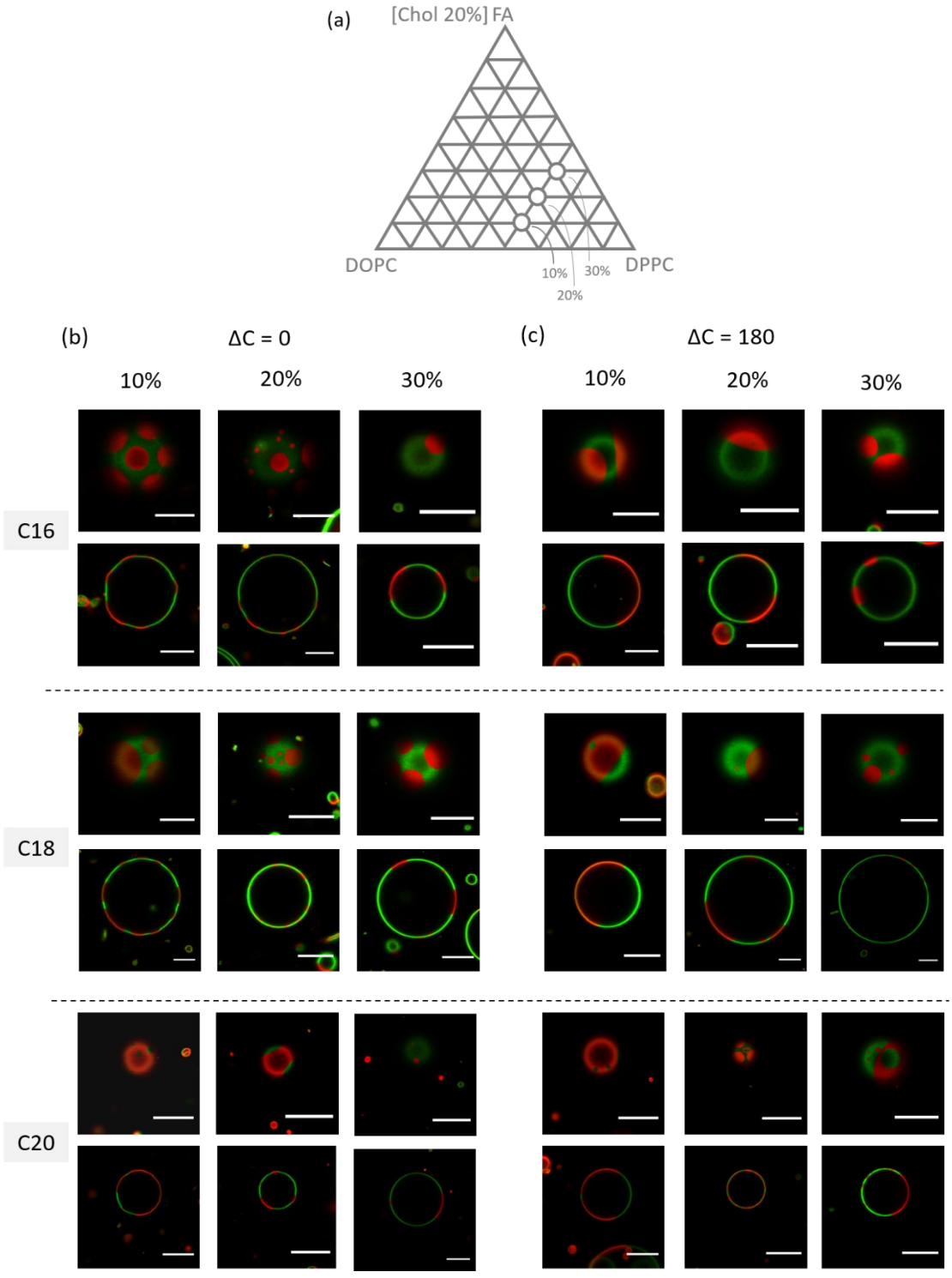
(a)
[Chol 20%] FA
DOPC
DPPC
10%
20%
30%
(b)
ΔC = 0
(c)
ΔC = 180
10%
20%
30%
10%
20%
30%
C16
C18
C20

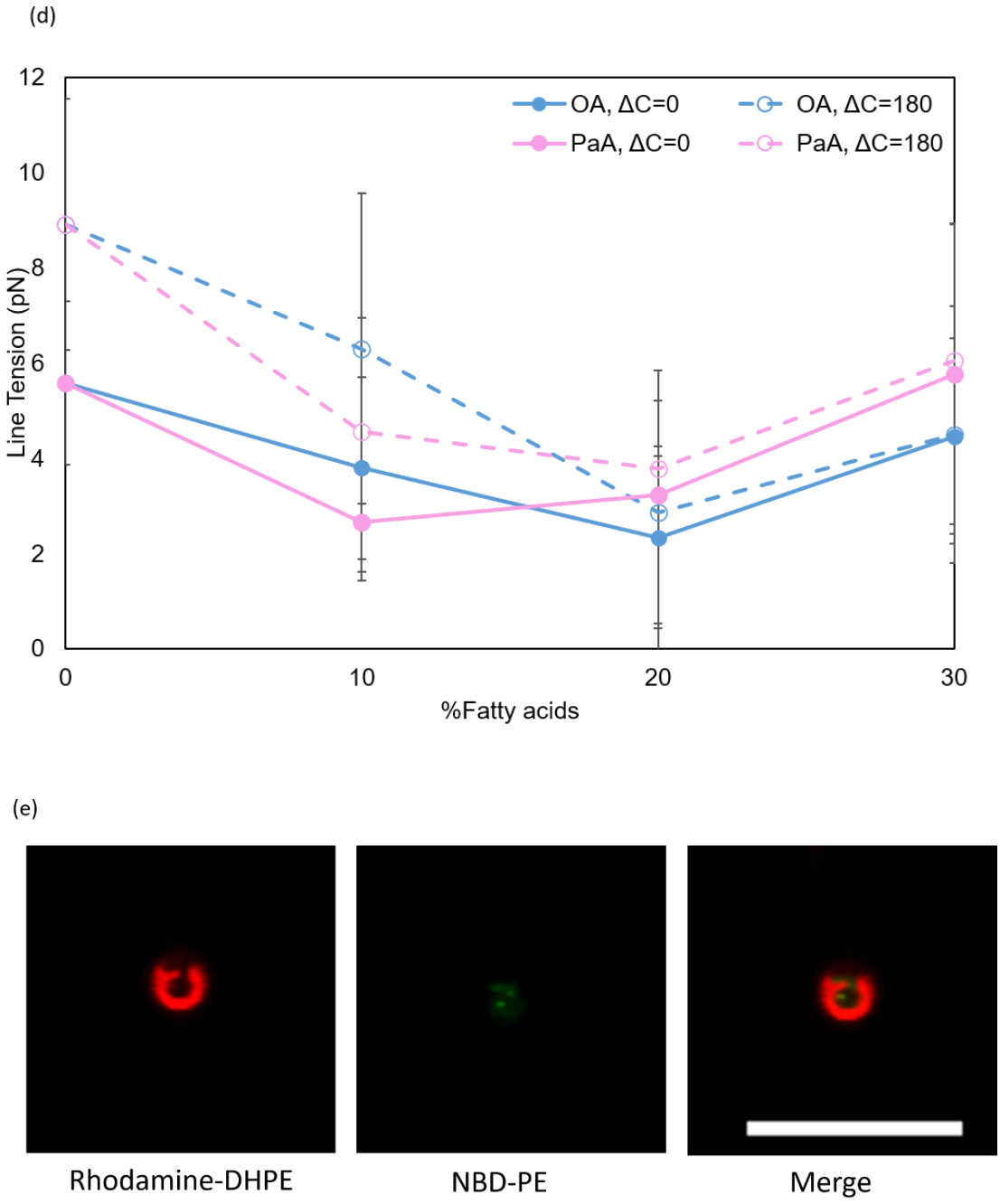

Figure 5-2 Confocal laser scanning microscopy images at composition of DOPC/DPPC/FA/Chol = 30/40/10/20 (10%); 20/40/20/20 (20%); and 10/40/30/20 (30%) of PA (C16), OA (C18), and EA (C20) without osmotic pressure (b) and with osmotic pressure (c). Scale bar: 10 µm. (d) Line tension at the L_o/L_d phase boundary in DOPC/DPPC/FA/Chol as a percentage of FA. (e) Images of S_o/L_d phase as the population of DOPC/DPPC/EA/Chol.

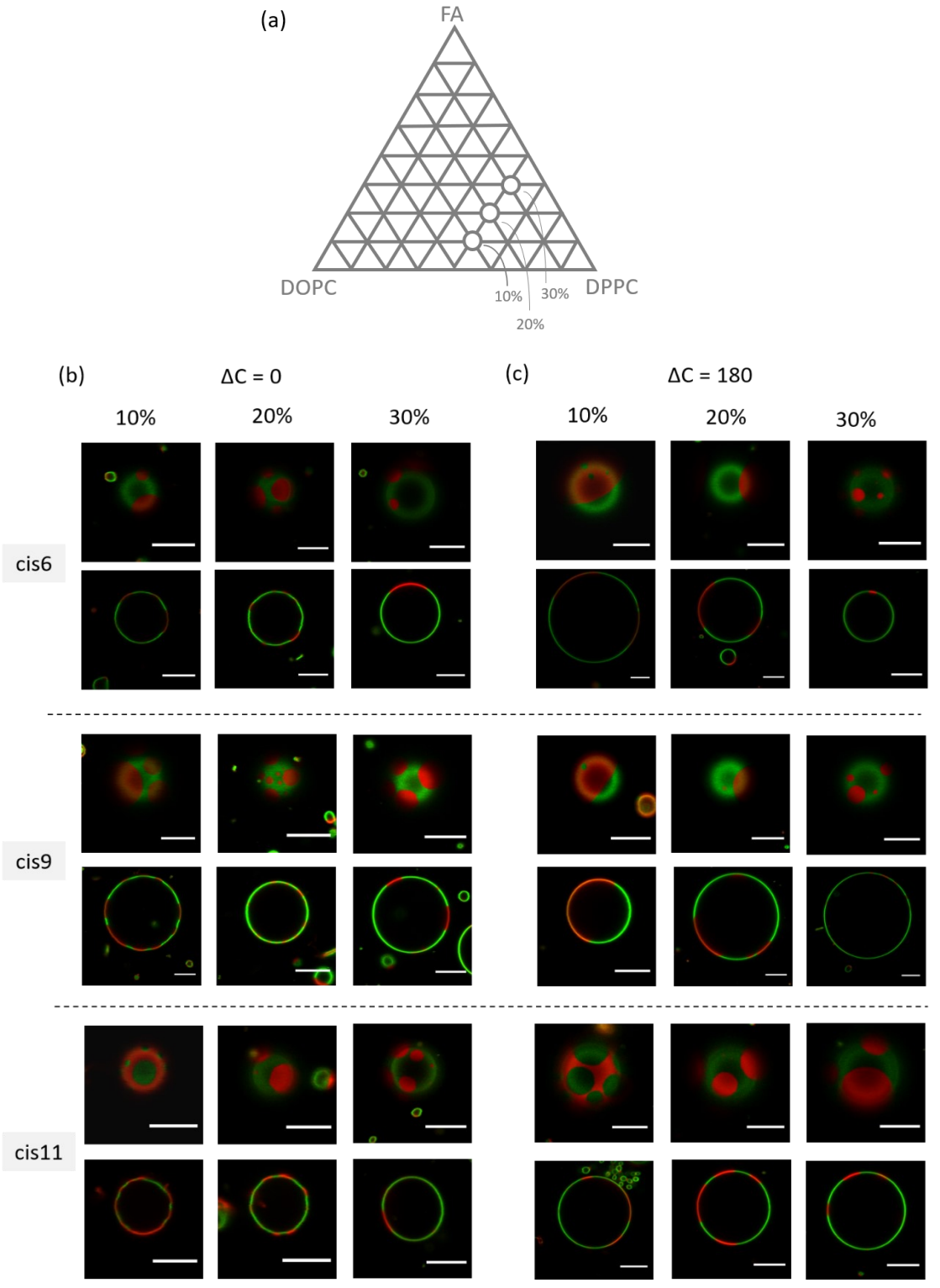
(a)
FA
DOPC
DPPC
10%
20%
30%
(b)
ΔC = 0
(c)
ΔC = 180
10%
20%
30%
10%
20%
30%
cis6
cis9
cis11

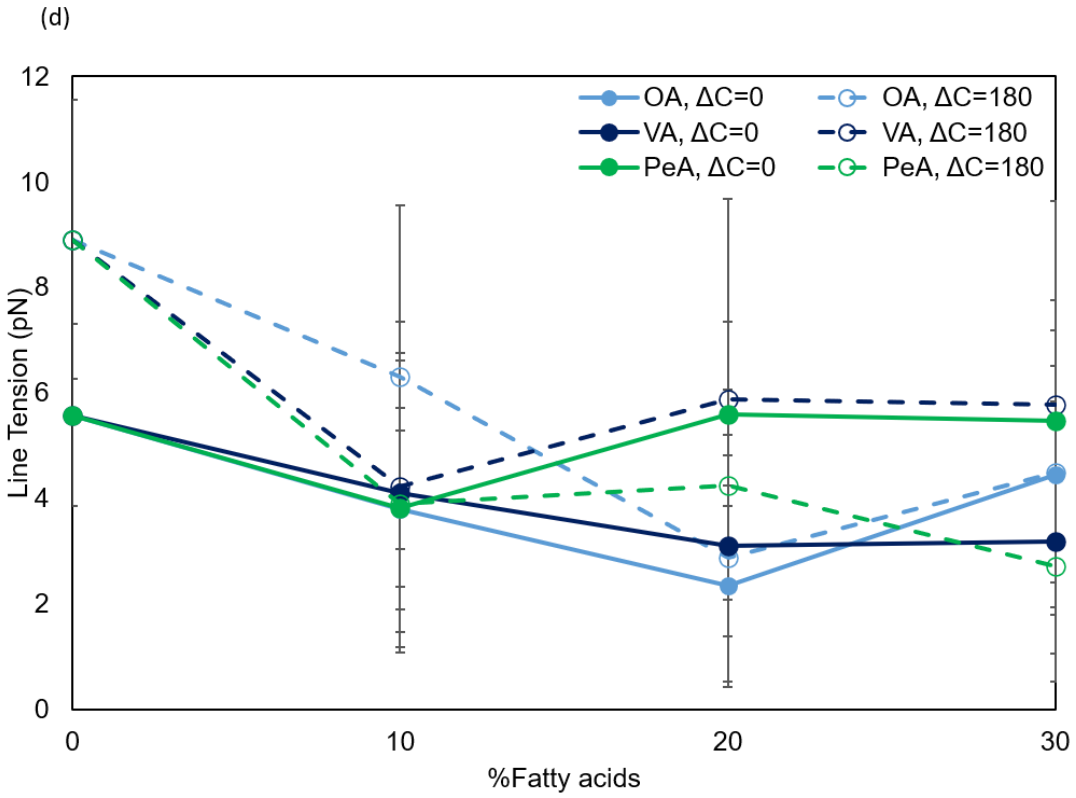

Figure 5-3 Confocal laser scanning microscopy images at composition of DOPC/DPPC/FA/Chol = 30/40/10/20 (10%); 20/40/20/20 (20%); and 10/40/30/20 (30%) of PeA (C18:1, cis 6), OA (C18:1, cis 9), and VA (C18:1, cis 11) in normal condition (b) and with osmotic pressure (c). Scale bar: 10 µm. (d) Line tension at the L_o/L_d phase boundary in DOPC/DPPC/FA/Chol as a percentage of FA.

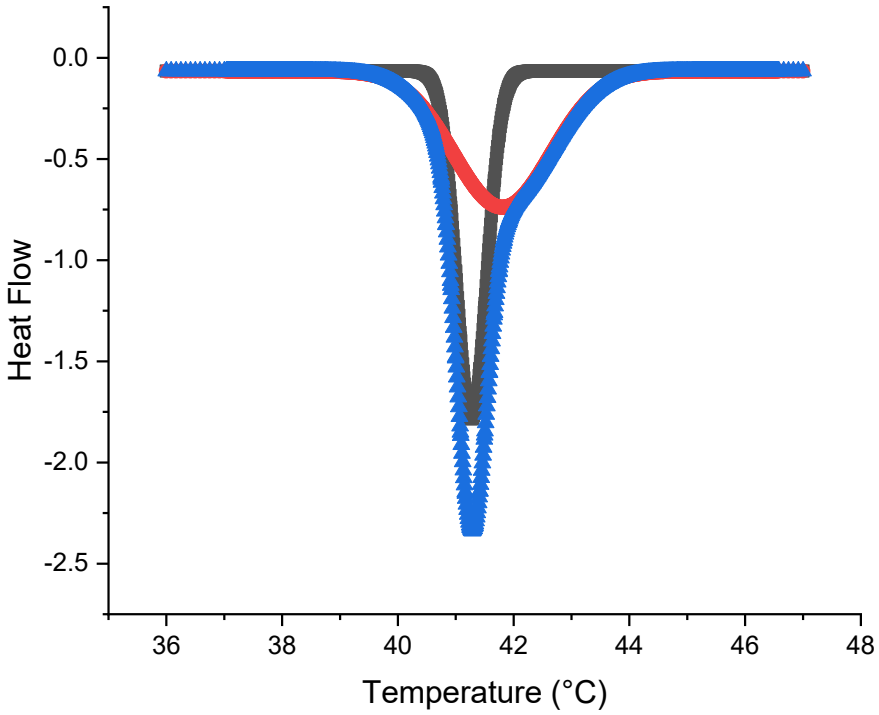

Figure 5-4 The fitting curve of DPPC/Chol 90/10. Blue line indicates the fitting curve of experimental results. Black and red lines are the curves for two independent transitions.

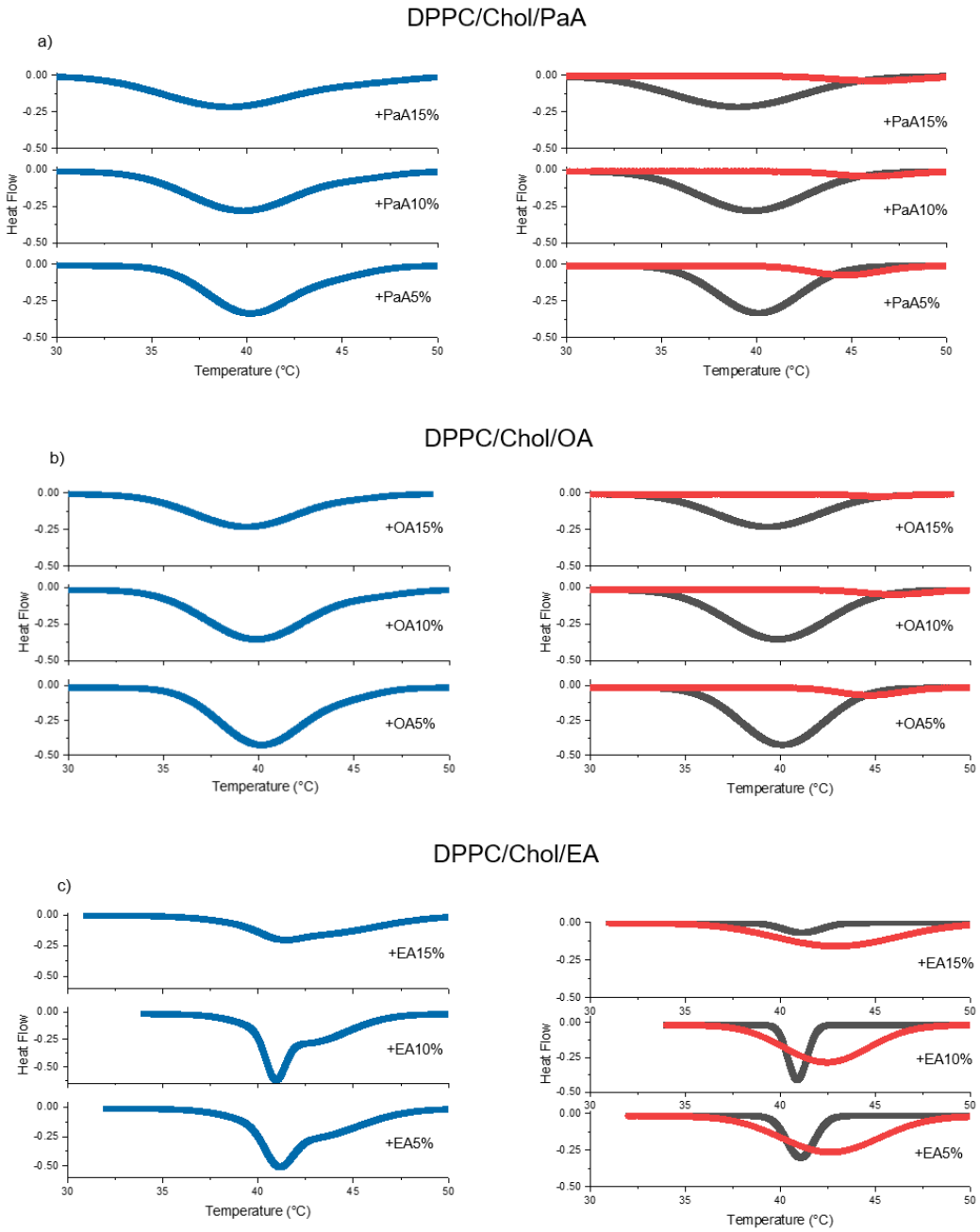

Figure 5-5 The obtained thermographs and the fitting curves of DPPC/Chol/PaA (C16:1, cis 9) (a), DPPC/Chol/OA (C18:1, cis 9) (b), and DPPC/Chol/EA (C20:1, cis 9) (c) with the additional of fatty acid at 5%, 10%, 15%, respectively. Blue line indicates the thermographs obtained experimentally. Black and red lines are the curves for two independent transitions obtained from peak deconvolution.

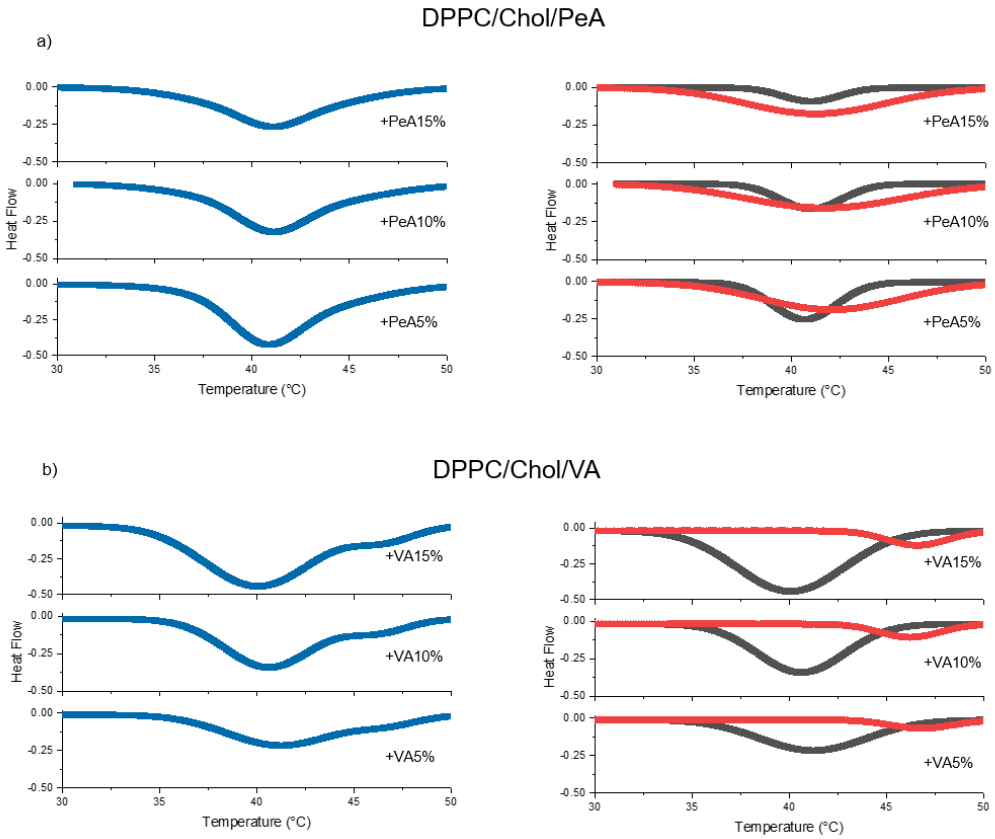

Figure 5-6 The obtained thermographs and the fitting curves of DPPC/Chol/PeA (C18:1, cis 6) (a), and DPPC/Chol/VA (C18:1, cis 11) (b) with the additional of fatty acid at 5%, 10%, 15%, respectively. Blue line indicates the thermographs obtained experimentally. Black and red lines are the curves for two independent transitions obtained from peak deconvolution.

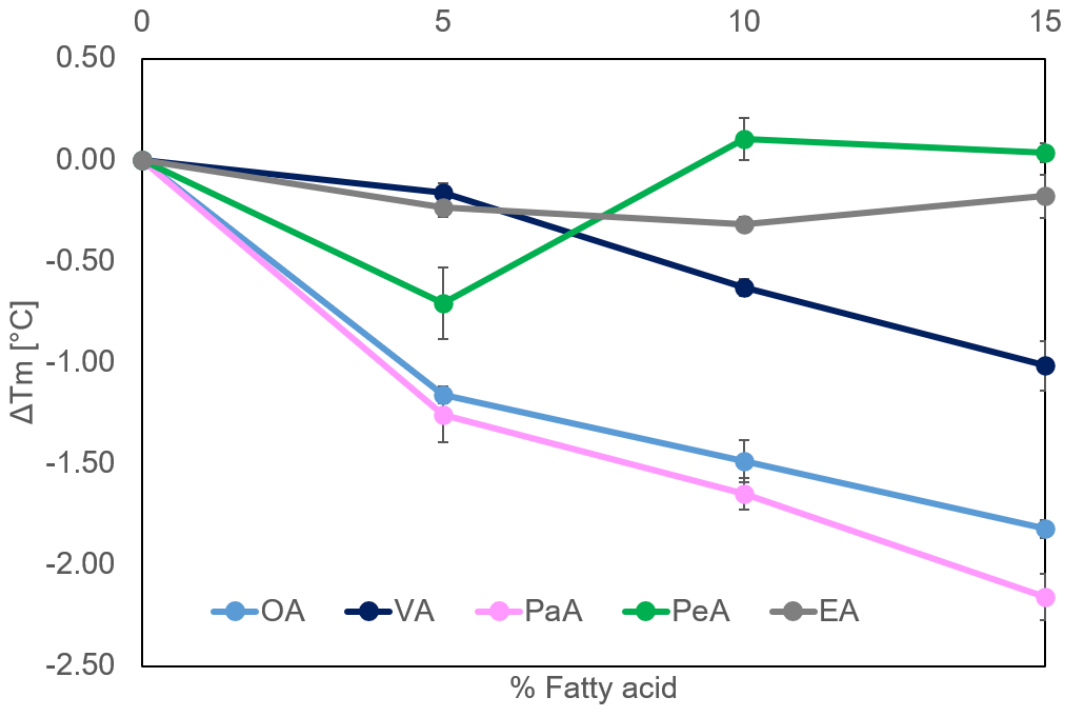

Figure 5-7 Averaged transition temperature difference ΔT_m as a function of fatty acid concentration.

Table 5-1 Fraction of fluctuated domain of each types of fatty acids

%FA	OA	PaA	VA	PaA
10%	40%	60%	57%	30%
20%	70%	25%	50%	0%
30%	10%	10%	40%	10%

Discussion

We presented the effects of varying chain lengths of fatty acids (C16, C18, and C20) and different cis position of fatty acids (cis6, cis9, cis 11) on the phase behaviors, line tension, and DSC thermographs. Results are compatible with the previous works (Shimokawa et al., 2017) in which suggested that OA, the monounsaturated (low melting temperature) fatty acid, normally partition in the L_d phase but some of them can also partition in the L_o phase and disrupt the hydrophobic chains of ordered phase. The difference in physical properties including chain ordering, membrane thickness, and spontaneous curvature between L_o and L_d phases is reduced. Therefore, line tension is reduced. Another branched-chain, phytanic acid (PhA) also has a lower melting temperature. It shared those behaviors as OA, so it was categorized as the Oleic acid types. Whereas the saturated (palmitic acid, PA) and trans configuration (elaidic acid, ElA) fatty acid exhibit differently by closely packed in the L_o phase and exclude cholesterol from the L_o phase. The L_o phase of vesicles containing these types of fatty acid is enhanced to turn to S_o phase. This behavior will be called as the Palmitic acid type. Based on the melting temperature of each fatty acid, and our results on their properties in partitioning, the line tension values, and DSC results, the fatty acids examined in this study can be classified into the Palmitic acid type or Oleic acid type.

OA (C18:1 cis 6) showed consistent results as the increase of OA content can suppress line tension, increase the amount of fluctuation domain, and decrease the transition temperature.

PaA (C16:1 cis 6) displays the shorter chain than OA (C18:1 cis9). DSC results of PaA are comparable to those of OA. Interestingly, as the increase in the concentration of PaA, the transition temperature is strongly reduced than those of OA. However, their line tension is suppressed less than OA. It can be implied that PaA provides a higher degree of disturbed the packing chain of L_o but it can incorporate in DPPC less than OA. The tendency of line tension is corresponding to the fraction of the fluctuation domain. Therefore, PaA can be classified as the Oleic acid type as they destabilize the L_o phase as shown in the decreasing of transition temperature and line tension value when increase content of PaA.

VA (C18:1 cis 11) is the isomer of OA with different in cis position. From DSC results of VA exhibited that VA is not well compatible with DPPC and cholesterol. They can form the VA-rich phase as a presence in the second peak in higher temperatures. This can be indicated that the interaction between VAs is very strong due to their long-chain structure. However, VA can destabilize the L_o phase as shown in the decreasing of the transition temperature. The line tension results are in agreement with DSC results. Line tension values are suppressed as increasing the content of VA. The suppressed line tension from the VA is not as much as those from OA. Based on the fraction of the fluctuation domain results, VA showed a highly disturbed L_o phase as OA. As VA can destabilize the L_o phase, it was categorized as the Oleic acid type. To improve these results, we have a future plan to increase the number of fluctuating domains to analyze.

Also, the melting temperatures of OA, VA, and PaA are 13°C, 14°C and -1°C, respectively. These temperatures are sufficiently lower than the chain melting

transition temperature for DPPC (42°C) and the miscibility temperature for DOPC/DPPC/Chol=40:40:20 (about 30°C). These also strongly support their behaviors as the disordered chain at room temperature as the disordered phase.

Based on the melting temperature, PeA (30°C) and EA (23°C) were classified as Palmitic acid type. Also, the longest kinked chain of PeA shares the same size as those of EA (11 carbon kinked tail).

The DSC and line tension results of PeA (C18:1 cis 6) are in agreement. As an increase in PeA concentration, the transition temperature and line tension showed a bit increase. This OA isomer also showed that it can well mix with DPPC and cholesterol. Even though PeA is the isomer of OA and VA, it has a higher melting temperature due to its double bond is in the even position (Hughes, Gunstone, 2012; Knothe & Dunn, 2009). When PeA forms crystalline conformation, it might more stable than the odd position, Therefore, its melting temperature is higher than OA and VA. Their high melting temperature similar to DPPC accordingly at room temperature observation, PeA does not disrupt the order phase as the Oleic acid type. In contrast, this unsaturated fatty acid does not provide properties to exclude cholesterol as palmitic acid since none of S_o/L_d was observed in vesicles containing PeA. PeA also has a kinked structure and may disturb the chain ordering of the L_o phase. The length between the double bond and the end of the hydrocarbon tail is long (the number of carbons is 12), and the melting temperature is higher than the other fatty acids. Therefore, PeA can form a relatively ordered structure than other fatty acids. When PeA is partitioned into the L_o phase, PeA disturbs the chain ordering of the L_o phase and excludes some amount of cholesterol. These two

effects offset each other. Therefore, the line tension values of PeA are the almost same as the values for control composition without any fatty acids. We conclude PeA has an intermediate property between the Oleic acid type and the Palmitic acid type.

Interestingly, EA (C20:1, cis9) produces two peaks on the thermograph results as VA but the second peak is very strong differently from VA. Therefore, EA tends to pack together with EA as the EA-rich phase. The EA-rich phase can destabilize the formation of liposome and also exclude cholesterol as the presence of S_o/L_d phase. Such the long hydrophobic chain cis unsaturated fatty acid (C20) of EA shared the same properties as the saturated and trans-unsaturated fatty acid (Shimokawa et al., 2017). The partition of EA in the L_o phase does not disturb the ordered chain. They attract to DPPC and exclude cholesterol. This effect is more pronounced for EA and we observed S_o phase in EA containing vesicles.

Our results showed that osmotic pressure produced from the hypotonic solution can enhance the line tension value. In DOPC/DPPC/Cholesterol, we proposed that the increase of line tension is from the reorganization of DOPC, DPPC, and cholesterol. Whereas in the fatty acid mixed DOPC/DPPC/Chol lipid membrane, it was also showed that the line tension can be enhanced upon the osmotic pressure by the reorganization of fatty acid from the L_o phase to L_d phase. In the OA (C18:1, cis9) system, 10% showed a higher increase in line tension of more than 20%. It can be implied that 20% might be the saturated amount of OA that can incorporate in the

L_o phase. Therefore, at 20% of OA containing, OA is more difficult to reorganize from L_o to L_d phase because there are so many OA molecules in the L_d phase.

PaA (C16:1, cis9) incorporates in the L_o phase less than OA but has a strong degree of disturbance to the L_o phase. Under osmotic pressure, 10% PaA can be reorganized PaA from L_o to L_d phase as OA. Whereas at 20% PaA, the major population of PaA tends to partition in the L_d phase so the enhance of line tension from the osmotic pressure is not as much as 10%PaA. The effect of the cis position of VA (C18:1, cis11) presented that a very small amount of VA includes in the L_o phase at 10%. The line tension obviously increases to 20%VA and 30%VA.

Interestingly, osmotic pressure suppressed line tension of PeA (C18:1, cis6) containing vesicles. We exclude EA from line tension analysis since the presence of the S_o/L_d phase. However, it was found that osmotic pressure can enhance the number S_o/L_d phase.

The important results are that osmotic pressure can increase the line tension by relocalization of fatty acids from the L_o phase to the L_d phase, but the tendency is not quite clear from line tension analysis. Since the line tension value calculated from the fluctuated domain, the high value of line tension under osmotic pressure was because the domains do not fluctuate. Therefore, these results should be improved and confirmed by fluorescent anisotropy to determine the degree ordering.

This study plan to further study the effect of osmotic pressure on the degree of ordering. Furthermore, the electric charge on hydrophilic carboxyl group, flip-flop

movement, and electrostatic formation might abet for fully understand the phase behavior of fatty acid-containing lipid membranes.

Reference

Cao, J., Schwichtenberg, K. A., Hanson, N. Q., & Tsai, M. Y. (2006). Incorporation and clearance of omega-3 fatty acids in erythrocyte membranes and plasma phospholipids. *Clinical Chemistry*, *52*(12), 2265–2272. https://doi.org/10.1373/clinchem.2006.072322

Cordomí, A., Prades, J., Frau, J., Vögler, O., Funari, S. S., Perez, J. J., Escribá, P. V., & Barceló, F. (2010). Interactions of fatty acids with phosphatidylethanolamine membranes: X-ray diffraction and molecular dynamics studies. *Journal of Lipid Research*, *51*(5), 1113–1124. https://doi.org/10.1194/jlr.M003012

Georgieva, R., Chachaty, C., Hazarosova, R., Tessier, C., Nuss, P., Momchilova, A., & Staneva, G. (2015). Docosahexaenoic acid promotes micron scale liquid-ordered domains. A comparison study of docosahexaenoic versus oleic acid containing phosphatidylcholine in raft-like mixtures. *Biochimica et Biophysica Acta - Biomembranes*, *1848*(6), 1424–1435. https://doi.org/10.1016/j.bbamem.2015.02.027

Hughes, Gunstone, F. D. (2012). Fatty acid and lipid chemistry. In *Journal of Chemical Information and Modeling* (Vol. 53, Issue 9). Springer.

https://doi.org/10.1017/CBO9781107415324.004

Hulbert, A. J., Kelly, M. A., & Abbott, S. K. (2014). Polyunsaturated fats,

membrane lipids and animal longevity. *Journal of Comparative Physiology B: Biochemical, Systemic, and Environmental Physiology*, *184*(2), 149–166. https://doi.org/10.1007/s00360-013-0786-8

Jump, D. B. (2002). The biochemistry of n-3 polyunsaturated fatty acids. *Journal of Biological Chemistry*, *277*(11), 8755–8758. https://doi.org/10.1074/jbc.R100062200

Killian, J. A. (1998). Hydrophobic mismatch between proteins and lipids in membranes. *Biochimica et Biophysica Acta (BBA) - Reviews on Biomembranes*, *1376*(3), 401–416. https://doi.org/10.1016/S0304-4157(98)00017-3

Knothe, G., & Dunn, R. O. (2009). A Comprehensive Evaluation of the Melting Points of Fatty Acids and Esters Determined by Differential Scanning Calorimetry. *JAOCS, Journal of the American Oil Chemists' Society*, *86*(9), 843–856. https://doi.org/10.1007/s11746-009-1423-2

Levental, K. R., Lorent, J. H., Lin, X., Skinkle, A. D., Surma, M. A., Stockenbojer, E. A., Gorfe, A. A., & Levental, I. (2016). Polyunsaturated lipids regulate membrane domain stability by tuning membrane order. *Biophysical Journal*, *110*(8), 1800–1810. https://doi.org/10.1016/j.bpj.2016.03.012

Onuki, Y., Hagiwara, C., Sugibayashi, K., & Takayama, K. (2008). Specific effect of polyunsaturated fatty acids on the cholesterol-poor membrane domain in a

model membrane. *Chemical and Pharmaceutical Bulletin*, *56*(8), 1103–1109. https://doi.org/10.1248/cpb.56.1103

Roach, C., Feller, S. E., Ward, J. A., Shaikh, S. R., Zerouga, M., & Stillwell, W. (2004). Comparison of cis and trans fatty acid containing phosphatidylcholines on membrane properties. *Biochemistry*, *43*(20), 6344–6351. https://doi.org/10.1021/bi049917r

Shimokawa, N., Mukai, R., Nagata, M., & Takagi, M. (2017). Formation of modulated phases and domain rigidification in fatty acid-containing lipid membranes. *Physical Chemistry Chemical Physics*, *19*(20), 13252–13263. https://doi.org/10.1039/c7cp01201b

Shimokawa, N., Nagata, M., & Takagi, M. (2015). Physical properties of the hybrid lipid POPC on micrometer-sized domains in mixed lipid membranes. *Physical Chemistry Chemical Physics*, *17*(32), 20882–20888. https://doi.org/10.1039/c5cp03377b

Smith, E. A., Smith, C., Tanksley, B., & Dea, P. K. (2014). Effects of cis- and trans-unsaturated lipids on an interdigitated membrane. *Biophysical Chemistry*, *190–191*, 1–7. https://doi.org/10.1016/j.bpc.2014.03.004

Soni, S. P., Ward, J. A., Sen, S. E., Feller, S. E., & Wassall, S. R. (2009). Effect of trans unsaturation on molecular organization in a phospholipid membrane. *Biochemistry*, *48*(46), 11097–11107. https://doi.org/10.1021/bi901179r

Stottrup, B. L., Heussler, A. M., & Bibelnieks, T. A. (2007). Determination of line

tension in lipid monolayers by fourier analysis of capillary waves. *Journal of Physical Chemistry B*, *111*(38), 11091–11094. https://doi.org/10.1021/jp074898r

McMullen, T. P. W., & McElhaney, R. N. (1995). New aspects of the interaction of cholesterol with dipalmitoylphosphatidylcholine bilayers as revealed by high-sensitivity differential scanning calorimetry. *BBA - Biomembranes*, *1234*(1), 90–98. https://doi.org/10.1016/0005-2736(94)00266-R

Wassall, S. R., Brzustowicz, M. R., Shaikh, S. R., Cherezov, V., Caffrey, M., & Stillwell, W. (2004). Order from disorder, corralling cholesterol with chaotic lipids: The role of polyunsaturated lipids in membrane raft formation. *Chemistry and Physics of Lipids*, *132*(1), 79–88. https://doi.org/10.1016/j.chemphyslip.2004.09.007

Wassall, S. R., & Stillwell, W. (2009). Polyunsaturated fatty acid-cholesterol interactions: Domain formation in membranes. *Biochimica et Biophysica Acta - Biomembranes*, *1788*(1), 24–32. https://doi.org/10.1016/j.bbamem.2008.10.011

Zaloga, G. P., Harvey, K. A., Stillwell, W., & Siddiqui, R. (2006). Trans fatty acids and coronary heart disease. *Nutrition in Clinical Practice*, *21*(5), 505–512. https://doi.org/10.1177/0115426506021005505

Chapter 6 Summary and conclusion

Summary

Chapter 2

Chapter 2 exhibits the entire ternary phase diagram of DOPC/DPPC/Chol in three specific temperatures. The responsiveness of each composition to the osmotic tension has also been plotted in the adjacent phase diagrams. Based on the reduction in temperature, the phase separation was enhanced which is the consequence of the high melting temperature (saturated) lipids are rigid and lateral more ordering at low temperature. While the low melting temperature (unsaturated) lipids are melted and lateral disordered in the membrane. Their state matters are much different at low temperatures. Increase temperature tends to melt the high melting temperature (saturated) lipids and become homogeneous when the temperature is higher than the melting temperature. Effects of temperature to phase separation have been discussed for decades. This study focused on responses of them to the osmotic tension. Our phase diagrams are clearly shown the enhancement of phase separation even in high temperature. The osmotic tension is generated by the application of the vesicles in a hypotonic solution. Consequently, membranes are allowed water efflux to inside the vesicles to homeostatically maintain is the isotonic state between in/out of membranes. These tensed membranes might thermodynamically induce the lateral reorganization and enhance the phase separation to occur.

Chapter 3

The effects of osmotic tension on the miscibility temperature are elucidated in this chapter. We compared results among various contents of cholesterol (0%, 20%, and 40%) and DOPC (10% and 20%). It was found that increase cholesterol content conduces to decrease the miscibility temperatures whereas decrease DOPC content conduces to increase the miscibility temperature. A more fluidity of the L_o phase results in a more decrease in miscibility temperature. Likewise, more content of high-melting temperature lipids determines higher miscibility temperature. Their miscibility temperature was shifted under osmotic tension. The shifted in the L_o phase is much higher than S_o phase. Therefore, cholesterol might play a role to shift the miscibility temperature under osmotic tension. The increase of cholesterol causing the more increase of fluidity if the L_o phase. The higher fluidity membranes commonly respond higher than the solidity membrane. These results additionally support the results in the previous chapter.

Chapter 4

Our results showed that osmotic tension repressed the fluctuation of membranes as shown in the line tension measurement by Flicker spectroscopy of domain boundary fluctuation. The osmotic tension induced the line tension from 0.4±0.3 to 1.2±1.2 pN in the DiphyPC system and from 0.6±0.3 to 1.8±0.5 pN in the DOPC system at room

temperature. We also proposed the plausible mechanisms behind it. Based on the free energy of the membrane, the degree of membrane undulation is inversely proportioned to the rigidity of the membrane. The application of osmotic stress to the soft membrane (L_d phase) suppressed the membrane fluctuation. This suppression is large in the L_d phase (homogeneous). Therefore, the homogeneous phase becomes unstable and energetically phase separation (forming L_o or S_o phases). When explaining in terms of free energy of phase separation, the employment of osmotic stress decreases the f_{und} to becomes negative. The phase separation energetically occurs. The f_{und} of S_o phase with high rigidity is more difficult to be negative than the L_o phase. Therefore, the L_o/L_d phase shows a larger response than the S_o/L_d phase.

Chapter 5

We showed the effects of hydrophobic chain length and cis position of unsaturated fatty acid in terms of partitioning in the DOPC/DPPC/Chol membrane. It was found that those fatty acids are mainly partitioned in the L_d phase and some molecule can also partition in the L_o phase. We can be classified the fatty acid as the Oleic type and the Palmitic type due to their partition in the L_o phase. For the oleic types, the unsaturated fatty acid (OA, C18:1 cis 9) normally incorporate to L_d phase as the loose order. However, some molecules are possible to include in the L_o phase and destabilize the L_o phase as shown in the reduction of line tension value and transition temperature. While

the decrease in size of the unsaturated fatty acid, PaA (C16:1 cis 9) showed higher degree disturbance of DPPC ordered (16:0 PC). However, the line tension results showed that the incorporation of PaA in the L_o phase is smaller. As the increased content of PaA, the line tension does not trend to decrease. As the increase cis position, VA also showed a higher degree of disturbance to the L_o phase than OA and PaA. Similar to PaA, VA incorporates in the L_o phase less than OA and probably less than PaA. DSC results showed that VA tends to interact with VA molecules because of the strong interaction between the longer carbon chain of cis 11. However, increase VA tends to decrease the line tension value. Since the melting temperature of PeA and EA is as high as the ordered phase, the partition of them in the order phase is different. From the line tension results, PeA containing vesicles showed a higher value of line tension. PeA is concluded as the intermediate type between the Oleic acid type and the Palmitic acid type. The participation of the longest chain EA (C20:1) is predominantly Palmitic acid type. They disrupted the formation of stable vesicles. Also, EA can exclude cholesterol from the L_o phase to appear as S_o phase. The response of EA under osmotic pressure, the S_o/L_d phase production is increased.

Conclusion

In this work, we modulate line tension using a physical stimulus, osmotic pressure, and chemical stimuli using five different monounsaturated fatty acids. We

presented the phase behavior vs. osmotic tension of the ternary phase diagram of DOPC/DPPC/Chol, at room temperature (24°C), lower temperature (10°C), and physiological temperature (37°C). Our results showed that osmotic tension can promote phase separation at any temperature level. The responses of the membrane to osmotic tension were confirmed by shifts of the miscibility temperature. Interestingly, cholesterol is a key factor in producing the phase separation and temperature shift with osmotic tension. Membranes with high contents of cholesterol (L_o phase) showed high values of temperature shifts, whereas those that lacked cholesterol (S_o phase) showed slight temperature shifts. Moreover, we found that the line tension at the L_o/L_d domain boundary was increased under the addition of osmotic pressure. The fluctuation results were also noted in a DiphyPC system and the vesicles containing fatty acids, in which fluctuation is noticeable. Furthermore, we also showed the modulation of line tension using different length and cis position of monounsaturated fatty acids. OA (C18:1 cis9), PA(C16:1 cis9), and VA (C18:1 cis11), can be classified as the Oleic type whereas PeA is the intermediate type. And EA is similar to the Palmitic type. Osmotic pressure can also reorganization of those unsaturated fatty acids and alter the line tension values. This work provides insights into the enhancement of phase separation in systems with various lipid ratios at a particular temperature, addition of unsaturated fatty acid different in length and cis position, and under osmotic pressure, which cannot be obtained in actual living cells. The results may contribute to a better understanding of the homeostasis of cells and lipid membrane itself might have the mechanosensory to

regulate the phase separation which can also regulate several mechanisms including the signal transduction, membrane trafficking, and cell homeostasis

Acknowledgement

I would like to express my very great appreciation to my supervisor Professor Takagi Masahiro for his invaluable, constructive, and constantly encourage pieces of advice during the expansion of this work. His support so generously has been very much appreciated.

Also, I would like to express a deep sense of gratitude to Associate Professor Dr. Hamada Tsutomu for his cordial support, invaluable information, and supervision, which helped me in completing this work.

Without constant guidance, supervision, and support from Dr. Shimokawa Naofumi, this work would not have been possible. His fruitful impressions gave me a lot of imagination, creativity, and understanding during the planning and development of these experiments.

For my pleasant life in Japan, additional gratitude is given to all of my friends in the Takagi laboratory and Hamada laboratory. Also, my special thankfulness extends to the researchers and the secretaries in both Takagi and Hamada laboratory.

I am truly grateful to the JAIST-SIIT-NSTDA collaborative and Monbukagakusho Honors scholarships for financial support throughout my study. I gratefully acknowledge Associate Professor Dr. Pakorn Opaprakasit for giving me the chance to study in JAIST.

Last but not least, I am deeply indebted to my parents, Mr. Supot Wongsirojkul and Mrs. Pachara Wongsirojkul for their love, provided me with strength, and supported me in difficult times, and also my brother, Mr. Wasan Wongsirojkul who inspired me and provided constant encouragement.

Publication list

- N. Wongsirojkul, N. Shimokawa, P. Opaprakasit, M. Takagi, and T. Hamada. (2019, Nov). Osmotic tension-induced membrane lateral organization, Oral presented at JAIST-SIIT-NSTDA 2019 workshop, Ishikawa, Japan.

- N. Wongsirojkul, N. Shimokawa, P. Opaprakasit, M. Takagi, and T. Hamada.. (2020, Mar). Osmotic pressure-induced phase separation in mixed lipids membranes, Poster presented at 75th Annual Meeting (2020) – The Physical Society of Japan, Nagoya, Japan

- N. Wongsirojkul, N. Shimokawa, P. Opaprakasit, M. Takagi, and T. Hamada. *Langmuir*, **36**, 2937-2945 (2020).